INFRARED SPECTRAL IMAGING ANALYSIS OF CARTILAGE REPAIR TISSUE

A Thesis
Submitted to
the Temple University Graduate Board

In Partial Fulfillment
Of the Requirements for the Degree
MASTER OF SCIENCE IN BIOENGINEERING

By
Madhuri Krishna Penmatsa
May 2011

Dr. Nancy Pleshko
Thesis Advisor
Dept of Mechanical Engineering
Temple University

Dr. Theresa A. Freeman
Committee Member
Dept of Orthopedic Surgery
Thomas Jefferson University

Dr. Bin Wang
Committee Member
Dept of Mechanical Engineering
Temple University

ABSTRACT

Articular cartilage is a homogenous tissue that provides frictionless movement between joints while withstanding repetitive physical stress. Once degenerated as a result of osteoarthritis or an injury, it has very limited capacity for self-repair. Recent research has focused on developing many new technologies for cartilage repair. The successful application of these strategies is limited in part to lack of techniques to evaluate tissue response to interventions. Assessment of the structural and molecular changes in the primary cartilage components, proteoglycan (PG) and collagen is critical to evaluate progress of the repair tissue. In the present study Fourier transform infrared imaging spectroscopy (FT-IRIS) was utilized to evaluate molecular changes in normal and degenerated cartilage in a rabbit model of repair. Parameters such as collagen integrity, type II collagen and proteoglycan are important factors in determining the biomechanical properties of articular cartilage, and are likely as important in determining functional competence of repair tissue. Histological evaluations are considered to be one of the most important methods for determining the quality of the repair tissue, but still do not predict clinical outcome. It is possible that a new tissue scoring system that considers molecular parameters in the repair tissue, along with the histological outcomes, will better predict clinical success of repair. ***The main goal of this study is to assess correlations between histological grading, immunohistochemical assessments of type I and II collagen, and FT-IRIS parameters, in cartilage repair tissue in a rabbit model.*** These data will provide the basis for a novel tissue scoring system using FT-IRIS parameters alone, or in conjunction with histological and immunohistochemical outcomes. This could yield better correlations with clinical outcomes that may lead to optimization of the cartilage repair process.

ACKNOWLEDGEMENTS

I would like to thank my advisor, Dr. Nancy Pleshko for her invaluable guidance, motivation and encouragement throughout my research work. The unending support she offered me kept me enthusiastic and made this work a memorable experience. I also appreciate the time she took to help me even during her busy schedules.

I would like to thank Dr. Theresa A. Freeman for her constant support and her valuable suggestions throughout this work. I would also like to thank Dr. Bin Wang for his valuable feedback and timely suggestions during this project.

I would like to express my gratitude to my friends Swapna and Vijay Harsha, Vamshi Gangupomu, Hari Charan Kamaraju, Chetana Sunkari, and Naveen Kammili for their cheerful encouragement and help in many ways. I am very thankful to the members of Tissue Imaging and Spectroscopic Lab including Mugdha Padalkar, Somaieh Moghadam, Beril Kavukcuoglu, Uday Preetham Palukuru, Megan O'Brien, Arash Hanifi and Alireza Hosseini for helping me and making my study at Temple a pleasant experience.

Finally I would like to thank my husband Krishna Mohan Pinnamaraju, my parents Venkata Narasimha Raju Penmatsa and Usha Rani Penmatsa, and my brother Murali Krishna Penmatsa for being a true source of inspiration and without whose love and encouragement I would not have made it to this point.

DEDICATION

This Thesis is dedicated to

My Husband, Mr. Krishna Mohan Pinnamaraju

for his unconditional love and support &

for being my constant strength.

TABLE OF CONTENTS

ABSTRACT ii

ACKNOWLEDGEMENTS iii

DEDICATION iv

LIST OF FIGURES vii

CHAPTER 1: INTRODUCTION 1

Articular Cartilage 1

Structure of articular cartilage 2

Background and Motivation: 4

Quantitative methods of evaluating articular cartilage repair: 9

Immunohistochemical staining: 12

Fourier Transform Infrared Imaging Spectroscopy 13

CHAPTER 2: HYPOTHESIS AND SPECIFIC AIMS 19

Hypothesis 1: 19

Aim 1: 19

Aim 2: 19

CHAPTER 3: MATERIALS AND METHODS 21

Animal Model 21

Tissue Preparation: 21

Histological Grading: 22

Nature of the predominant tissue: 22

Surface regularity: 23

Structural integrity 23
Freedom from cellular changes of degeneration: 24
Bonding to the adjacent cartilage: 24
Immunohistochemical Staining 24
Image Analysis and Quantification of Collagens: 25
FT-IRIS Data Acquisition: 26
Infrared Imaging Analysis: 27
CHAPTER 4: STATISTICAL METHODS 30
CHAPTER 5: RESULTS 32
Histological results: 32
Immunohistochemistry: 33
Infrared imaging results: 34
Correlations 37
Regression Analysis 40
CHAPTER 6: DISCUSSION 42
REFERENCES CITED 47
APPENDIX 57
Appendix A: Protocols 57
Alcian blue and Hematoxylin staining 57
Deparaffinization 57
Alcian Blue and Hematoxylin Staining 57
DAB Immunohistochemistry protocol 58
Appendix B: Histological and Immunohistochemical Images 63
Appendix C: IR Images 69

LIST OF FIGURES

Figure 1: Schematic representation of the general structure of adult human articular cartilage to show the zones, regions, and relationship with subchondral bone. The insets show organizations of collagen macro fibrils in the different zones [5] 3

Figure 2: A normal and osteoarthritic joint [7] 4

Figure 3 : The Electromagnetic Spectrum... 13

Figure 4 : Primary absorbances of collagen and aggrecan in cartilage 16

Figure 5 : Spectrum of primary absorbances in cartilage. 17

Figure 6 : Infrared imaging spectral parameters in repair tissue 29

*Figure 7 : Histological score averaged per group (~ n = 5) graded by two independent observers * p < 0.05. .... 32*

Figure 8 : Progression in repair tissue quality, histological grade and its corresponding amount of type I and type II collagen staining at 2, 12 and 16 weeks repair.................. 34

*Figure 9 : Graphs from FT-IR analysis, Collagen, proteoglycan, collagen integrity and proteoglycan ratio to amide I averages per group were plotted (~n=5) significant differences p <0.05 were shown with ▼ repair at different time pointss, and with a * between repair and normal... 35*

*Figure 10 : Percentage of collagen fibrillar orientation averages per group (n ~ 5) * p < 0.05.. 36*

Figure 11 : Correlations of IR derived parameters to histological grade and type I and type II collagen based on group average values. a) Nature of the predominant tissue grade vs IR derived PG b) Proteoglycan staining grade vs IR derived PG c) Nature of the predominant tissue grade vs IR derived collagen d) Structural integrity grade vs IR derived collagen integrity e) Staining intensities of type II collagen with IR derived collagen content (amide I) f) Type I collagen staining vs IR derived collagen. g)Histological total score vs IR derived PG h) Histological total score vs IR derived collagen content.. 39

CHAPTER 1: INTRODUCTION

Articular Cartilage

Articular cartilage is a complex connective tissue composed of chondrocytes embedded within an organized extracellular matrix. The matrix contains an extensive network of collagen fibrils, which confer tensile strength, and an interlocking mesh of proteoglycan, proteins with covalently attached sulfated glycosaminoglycan molecules. Chondrocytes are the sole cellular components of adult hyaline cartilage and are responsible for synthesizing and maintaining the highly specialized cartilage matrix macromolecules. Hyaline cartilage consists predominantly of type II collagen and smaller amounts of type V, VI, IX, X, XI, XII, and XIV collagen [1]. It is translucent and bluish white in appearance. In hyaline cartilage, the chondrocytes reside in lacunae surrounded by a pericellular matrix. Articular cartilage is an avascular, aneural, alymphatic tissue nourished by diffusion from the vasculature of the subchondral bone and to lesser degree from the synovial fluid. Type II collagen constitutes 90% to 95 % of total collagen and 10 % of the wet weight. Type II collagen is the major fibrillar collagen of articular cartilage. It forms a highly cross linked and interconnected network of collagen fibrils. Type VI collagen forms as micro fibrils and is localized around Chondrocytes may play a role in cell attachment [2]. Types IX and XI are cartilage specific, these collagens are the minor types and are present in roughly equal amounts Type IX is a short fibrillar collagen that contains a proteoglycan moiety that forms cross-links with type II collagen, functions as an intermediate between type II collagen and proteoglycan aggregates in the extracellular matrix [3].

Structure of articular cartilage

Articular cartilage is structurally divided into three zones, each with a unique cellular morphology and arrangement of the type II collagen fibers (Figure 1). Chondrocytes in the most superficial or tangential zone are flattened, with collagen fibrils arranged parallel to the surface. In the other zones, chondrocytes maintain a characteristic round shape. The intermediate, or transitional, zone is the thickest. In this region, the collagen fibers are less organized but are typically in an oblique orientation to the surface. In the deep, or basal, zone, chondrocytes and collagen fibers are oriented in vertical columns perpendicular to the surface. Cellular density and water content is highest at the superficial layer of the articular cartilage and progressively decreases through the intermediate and deep zones to about one-third the density of the superficial layer. The proteoglycan content is the lowest in the superficial zone and progressively increases through the middle and deep zones [4]. The composition and structural organization of articular cartilage in the human adult reflects the very specialized role of this tissue in articulation.

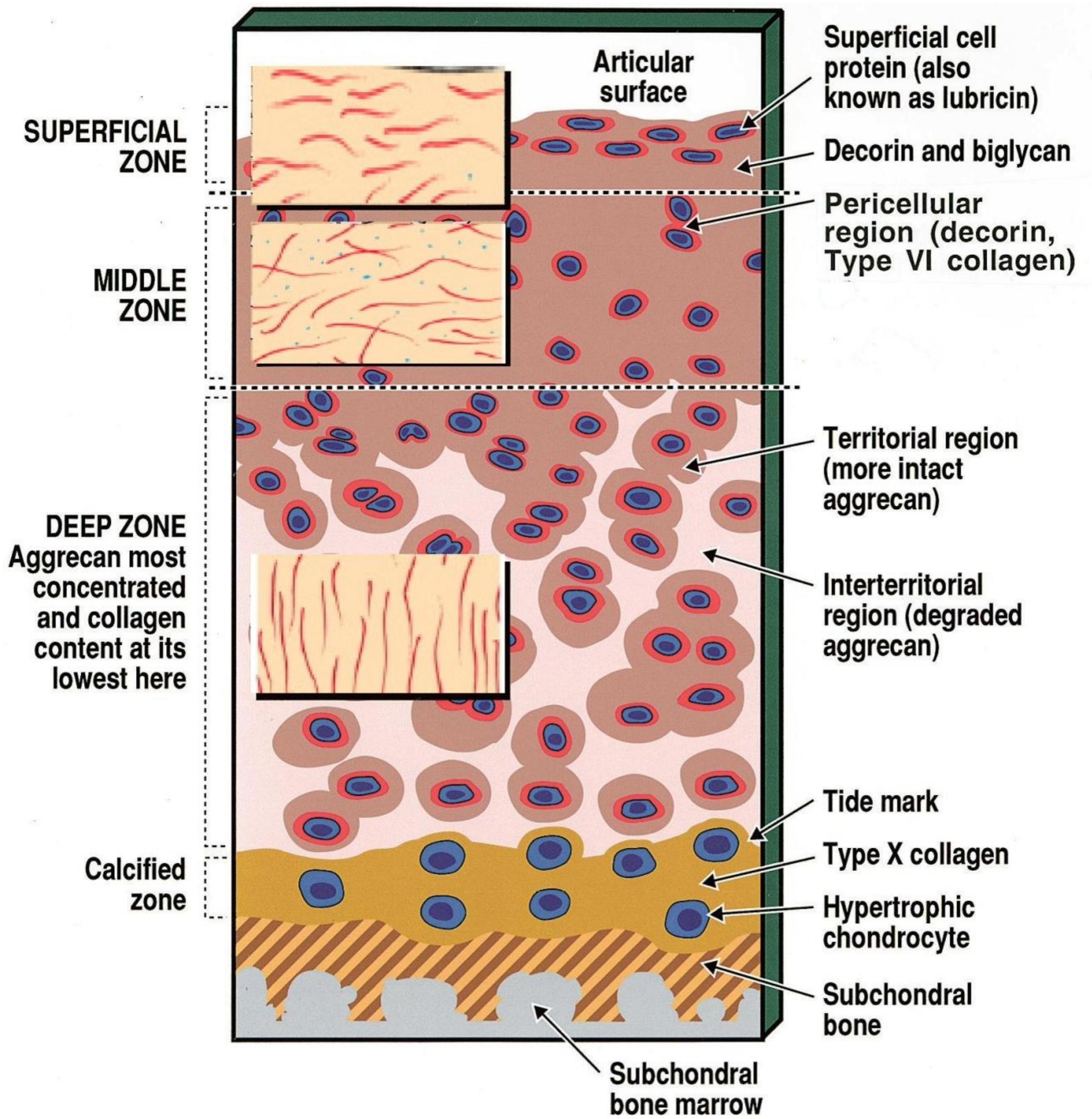

Figure 1: Schematic representation of the general structure of adult human articular cartilage to show the zones, regions, and relationship with subchondral bone. The insets show organizations of collagen macro fibrils in the different zones [5]

Background and Motivation:

Chondrocytes undergo metabolic changes as a result of aging, disease, and injury. These changes may delay the tissue maintenance and repair, resulting in accelerated loss of articular surface and leading to end-stage arthritis. Chondrocytes maintain a balance between matrix synthesis and breakdown that facilitates normal tissue metabolism. This process is further influenced by several factors, including the mechanical load, hormones, local growth factors, cytokines, aging, and injury. Articular cartilage defects are often associated with loss of matrix components, increased water content and disruption of collagen fibrils. Some of the pathological changes include subchondral bone thickening, deformation of the articular surface, osteophyte formation, and synovial fibrosis, key features that often lead to osteoarthritis (Figure 2), one of the most prevalent joint diseases in the world and one of the leading causes of disability and pain in the elderly. [6] This complexity of the interaction between the cells, the extracellular matrix, and other factors makes in vitro reproduction of articular cartilage extremely difficult.

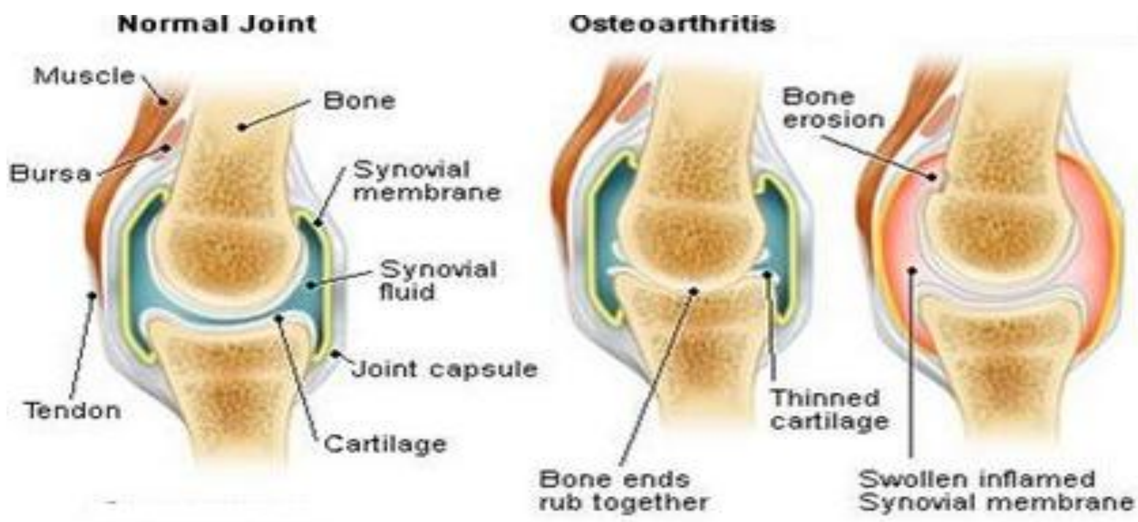

Figure 2: A normal and osteoarthritic joint [7]

It has been estimated that over 600,000 procedures are performed in the United States each year to repair damaged cartilage. Numerous experimental and clinical attempts to treat articular cartilage defects have been made, including drilling, abrasion chondroplasty, microfracture, abrasion arthroplasty, Autologous chondrocyte implantation, autograft and allograft techniques [1, 8, 9]. Many of these techniques result in fibrous tissue. Especially in full thickness defects, when the subchondral bone is also damaged, the repair response originates from the subchondral bone and results in fibrocartilage. Fibrocartilage, unlike hyaline, primarily consists of type I collagen and is fibrous in nature, and lacks the biomechanical properties, structure and composition of hyaline cartilage [10, 11].

The technique of microfracture works by stimulating the growth of new articular cartilage by creating a new blood supply. A sharp tool is used to make multiple holes in the subchondral bone that eventually creates a healing response. New blood supply can reach the joint surface, bringing newly generated chondrocytes that forms the new cartilage. This is very similar to subchondral drilling, which consists of drilling through the defect to penetrate the subchondral bone. Subsequent findings suggest the repair tissue introduced into the area can grossly appear like hyaline cartilage but histologically resembles fibrocartilage [4].

Abrasion arthroplasty is also similar to drilling. Instead of drills or wires, high speed burrs are used to remove the damaged cartilage and reach the subchondral bone. The technique works by debriding the articular defect to a normal tissue edge so that fresh collagen can be produced in the fibrin clot [1].

Soft tissue and osteochondral grafts: Stimulating articular cartilage growth through the use of various grafting techniques has recently been reported. Osteochondral transplantations involve harvesting a bone-cartilage graft from a non-weight bearing surface of the bone and transplanting it into the defect. Studies have reported good results with reduction of symptoms and improvement of function in short term observations [1, 12].

In contrast to the above described procedure, autologus chondrocyte implantation (ACI) is a two-step procedure. The process involves obtaining a biopsy from a non-load bearing region of the patient's articular cartilage. The chondrocytes are then released from the tissue by enzymatic digestion and expanded in culture. At a subsequent surgery a few weeks later, the cultured cells are implanted into the chondral defect, beneath a periosteal patch. This stage of the procedure requires an open arthrotomy of the knee to secure the patch to the surrounding normal cartilage. Results obtained showed reduced pain and restored joint function in many of the patients [11, 13].

Although many of the above stated techniques can result in symptomatic pain relief and improvement in functional status, many of these techniques fail to prevent future degeneration of the repair tissue and the surrounding host tissue. Degeneration is in part due to the nature of the repair tissue formed, such as fibrocartilage, inadequate development of quantity of repair tissue, poor cell differentiation and poor bonding to the surrounding articular cartilage [14].

.

Subchondral bone marrow stimulation techniques and cartilage penetration techniques, such as previously described microfracture, have recently received increased attention [15, 16]. The main aim of these procedures is to mobilize the mesenchymal stem cells to differentiate into cartilaginous repair tissue. The vascularized bone is disrupted to form a fibrin clot and thereby introducing pluripotent cells into the surrounding area. These stem cells eventually differentiate into chondrocyte cells that secrete type I, II and other collagen types, as well as cartilage specific proteoglycans, after receiving mechanical and biological cues. These stem cells typically produce a fibroblastic repair tissue that on visual appearance and initial biopsy can have a hyaline-like quality. Unfortunately, over time, the histological characteristics change into more predominantly fibrocartilaginous tissue [16].

Research from the past two decades has focused on investigating both normal and pathologic cellular and molecular processes, as well as the development of chondro-protective agents to improve the metabolic function of articular cartilage. Current research includes elucidation of the mechanism of actions of a variety of agents, such as glucosamine, chondroitin sulfate, and hyaluronic acid, and how they can modify the symptoms and course of osteoarthritis [12]. Methods of stimulating repair or replacing damaged cartilage, such as matrix metalloproteinase inhibitors, gene therapy, growth factors, cytokine inhibitors, artificial cartilage substitutes, tissue engineering, the combination of artificial matrices with cells and growth factors or genes, are currently under investigation and are thought to offer great potential for improving patient care [15].

With the development of several new treatment approaches, the need for objective outcome measures and the assessment of the repair tissue has become increasingly important. Especially, with regard to the development of new treatments for large cartilage defects, it is very valuable for orthopedic surgeons and researchers to understand how the initial repair tissue progresses to the competent repair tissue, and also to assess whether the repair tissue is developing as desired [12].

Therefore, animal models are frequently used to enable more controlled evaluation of the repair process. These models have the advantage that besides having tissue from known time points, normal healthy cartilage can also be obtained from the same subject. The most commonly used animal models to assess cartilage repair are rabbit [17-23] goat[24-26] , sheep [27, 28], dog, [29] and pig [30-32]. Depth of the defect may vary depending on the animal used, its maturity and its healing response. Spontaneous repair of full thickness defects is proven to occur in rabbits [33, 34]. Spontaneous repair of full thickness cartilage is associated with a series of physiological changes such as localized bleeding, hematoma formation, stem cell migration, and a variety of growth factors which influence the chondrocyte like cell formation. However, similar to what occurs in humans, these series often end up synthesizing type I collagen resulting in fibrocartilage [11, 35].

Nonetheless, studies have shown good to excellent histological repair in the absence of any specific treatment in animal models, and similar findings are supported by data from some clinical studies in humans as well [13, 36]. Based on these studies it is clear that the inter-individual variations of the response to cartilage defects strongly contribute to the outcome of the repair processes. The mechanism of spontaneous repair and the series of changes that occur physiologically during the process are important in understanding surgically based strategies, and for research investigations [1, 4]

Quantitative methods of evaluating articular cartilage repair:

The standard semi-quantitative methods to evaluate the repair tissue in articular cartilage are histology, biochemistry, and mechanical properties. Histological methods are widely used by researchers to evaluate cartilage repair, which allows assessment of many important factors in the repair process such as morphological, structural and cellular characteristics based on a scoring system. Factors included are type of tissue filling the defect (hyaline or fibrocartilage), including cells and extracellular matrix, the structural features, type of cells present and even the health of adjacent tissue. Assessment of morphological or biochemical information depends on the type of tissue, the method of staining and the scoring system. For instance, several histological stains are specific to sulfated glycosaminoglycans (GAGs) such as Safranin O and Alcian blue, while immunohistochemical stains are used to demonstrate the type of collagen and cartilage-specific proteins [37, 38].

In histological studies, the morphological appearance of the repair tissue is likely to be predictive of its functionality and durability. Many scoring systems have been developed in order to make the histological observations objective, and to some extent quantitative. While there are a wide variety of scoring systems available, only a few of them are validated. Some of them are validated by comparing to an already validated score, while some others have been validated by a biochemical analysis of the parameters [39]. Usage of validated scoring systems improves reliability of observations. The choice of the grading system may depend on the type of the tissue, and the characteristics that need to be assessed. Also some of these scoring systems have been validated for a specific tissue type, like the Bern score has been validated for an engineered cartilage [40], modified O'Driscoll score for in-vivo repaired cartilage [41], histological and histochemical grading system for an osteoarthritic cartilage, and ICRS II and OsScore for human repair tissue [39].

A variety of tissue characteristics can be assessed by a scoring system [39]. O'Driscoll score was the first cartilage repair score used to assess the quality of repair tissue in rabbits after periosteal grafting of cartilage [42] This was later modified to include cellularity, chondrocyte clustering and freedom from cellular changes of degeneration and now is referred to as the modified O'Driscoll score [43]. It is specific for cartilage repair and includes four major categories, the nature of the predominant tissue, structural characteristics, surface regularity, freedom from cellular changes of degeneration and freedom from degenerative changes in adjacent cartilage, and is frequently used for cartilage analysis in animal studies [42]. This score has recently been validated by correlating to the Pineda scale, and a high intra-and inter-observer reproducibility was demonstrated when used to analyze goat articular cartilage [41]. The O'Driscoll score is one of the few scores in which 'integration' of the repair tissue with its surrounding tissue is assessed.

Study of articular cartilage repair in human is somewhat different from the animal repair tissue. The assessment of human repair tissue is often limited by availability and size of the biopsy of the repaired tissue. As parameters like 'bonding to adjacent cartilage" from the O'Driscoll scoring system may not be useful for human tissues, as it can be scored only when a biopsy is taken from a transitional zone along with an adjacent native tissue at both ends thus requiring for a large biopsy, or a full joint explants. Harvesting large size biopsies from patients is not always desirable. Considering this issue, a new cartilage scoring system was developed, known as OsScore, for small biopsies of human samples [13]. The subsequently developed 'OsScore' comprises seven parameters ('tissue morphology, matrix staining, surface architecture, chondrocyte clusters, mineral blood vessels and basal integration.) and has a maximum score of 10 points [13].

The histology working group of the International Cartilage Repair Society (ICRS) had developed and validated a new scoring system that is suitable for human samples. This ICRS II score comprises of tissue morphology, cell morphology, and matrix staining metachromasia, architecture of the surface, basal integration, subchondral bone abnormalities, abnormal calcification, and vascularization within the repair tissue [44]. Similar to most other cartilage repair scores, this score does not evaluate integration of the repair tissue with its surroundings, which is due to the limited size of biopsy in the clinical setting.

Immunohistochemical staining:

The knowledge of molecular changes at the tissue level has improved vastly due to the application of immunohistochemical staining. Immunohistochemical staining can be applied to an unlimited number of targets, since specific antibodies can be generated against every protein or peptide. With respect to cartilage, a considerable number of antigens can be used in order to identity and localize specific structures. These antigens can be used to identify cellular or extracellular targets.

Immunostaining techniques work based on the general principle of antigen, antibody reaction. This process involves the localization of antigens in tissue sections by the use of a labeled antibody as specific reagents through antigen-antibody interactions that are visualized by a marker. The complexity of antigen and antibody can be visualized by binding the antibody via its invariable end to a secondary system. This is possible because site-specific protein structures serve as targets for the secondary system (for example primary antibodies generated in rabbits can be localized by an anti-rabbit secondary system). An appropriate enzyme (e.g. peroxide or alkaline phosphatase) can detect the resulting primary-secondary antibody complex The enzyme coupled to the secondary antibody provides a color reaction when appropriate substrates are added [38] The most commonly utilized antibodies in cartilage repair tissues are the monoclonal antibodies and polyclonal antibodies depending on the animal model. Monoclonal antibodies against type I and type II are widely used due to their specificity in binding to antigens. Several studies have used these antibodies to identify regions of hyaline and fibrocartilage tissue in human and animal tissues of cartilage repair [45, 46].

While assessment of the histological quality and immunohistochemical features of cartilage are considered to be important tools to identify pathological changes of cartilage and success of treatment, it is challenging to obtain quantitative information on the spatial distribution of tissue chemistry, which could be an important indicator of clinical success in repair. Fourier transform infrared imaging spectroscopy is a novel alternative to analyze structural, compositional and zonal variations in cartilage based on molecular information.

Fourier Transform Infrared Imaging Spectroscopy

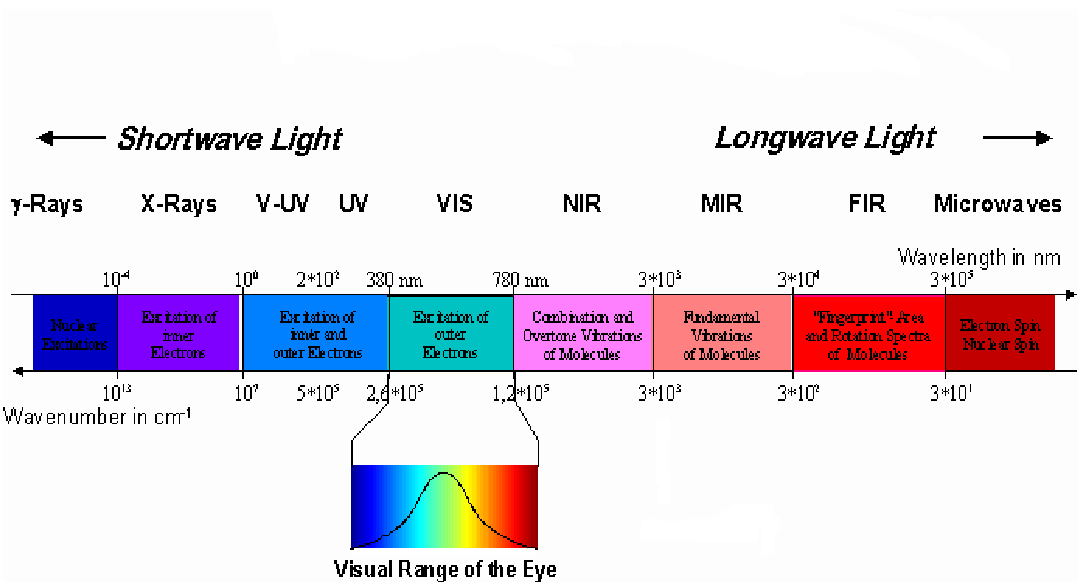

Figure 3 : The Electromagnetic Spectrum

Infrared spectroscopy is the study of the interaction of infrared light, composed of electric and magnetic waves, with matter (Figure 3). All objects in the universe at a temperature above absolute zero give off infrared radiation. When infrared light passes through a sample, certain frequencies of the light are absorbed by the chemical bonds thus leading to molecular vibrations in the substance. Hence the presence of chemical bonds in a material is a necessary condition for infrared absorbance to occur. Structural fragments molecules, known as functional groups, absorb specific frequencies that are characteristic to their structure. In infrared spectroscopy, frequency is typically measured in wave numbers, cm^{-1}. For instance the C = O stretch of a carbonyl group occurs at ~1700 cm^{-1} in ketones, aldehydes and carboxylic acids. Therefore, there is a correlation between the wave number at which a molecule absorbs infrared radiation and its molecular structure. Absorbance bands in the infrared arise from the primary molecular vibrations such as stretching and bending of molecules. This correlation between the frequencies and the molecules of a substance allows the identification of the structure from the infrared spectrum of molecules. The absorption pattern of each molecule is unique since the frequencies and intensities of absorbed infrared light depend on the specific bond strengths and atoms within the molecule. A plot of measured infrared radiation intensity versus wave number is known as an infrared spectrum, a powerful tool for both qualitative and quantitative analysis [47]

In addition to chemical structures, infrared spectra can provide quantitative information, such as the concentration of a molecule in a sample. The basis of quantitative analysis in infrared spectroscopy is based on Beer's law, which relates concentration to absorbance

$$A = € L c$$

Where A is absorbance

€ is absorptivity

L is pathlength

c is concentration.

The absorbance is measured as peak height or peak area, from the infrared spectrum. The absorptivity is the proportionality constant between concentration and absorbance. The molecules absorb infrared radiation at characteristic to their vibrational frequencies, enabling identification and quantification of components, Absorptivity is a material characteristic and it changes from molecule to molecule, and from wave number to wave number for a given molecule. The width of an infrared band gives information about the strength and nature of molecular interactions [48].

Fourier transform is the operation that decomposes a signal into its constituent frequencies. A Fourier Transform is required to turn the raw data into a spectrum. Fourier transform infrared (FTIR) spectroscopy is advancement in spectroscopy that combines infrared spectroscopy with the Fourier transform technique, thus permitting faster data acquisition. The goal of FTIR spectroscopy is to determine how well a sample absorbs or transmits light at each different wavelength. FTIR spectroscopy was developed to measure all of the infrared frequencies simultaneously, rather than individually. An FT-IR spectrometer in combination with an optical microscope, infrared imaging, can detect the molecular nature, distribution and orientation of the components of connective tissues on very thin tissue sections [49]. The system typically consists of an optical microscope with an array detector that has the capability to image a rectangular sample size up to several millimeters in length at a spatial resolution of 6.25µm or at 25µm [50]. FT-IR imaging spectroscopy typically utilizes the frequency of the mid-infrared region (4000-400cm^{-1}). The frequency at which a molecule absorbs infrared radiation is sensitive to conformation and infrared spectroscopy can be used to obtain information on protein secondary structure, and when polarized, an orientation of specific molecular bonds [51]. FTIR imaging spectroscopy (FT-IRIS) imaging has been widely used to analyze the biological cells and tissues [52-54]. In tissues, the structure and orientation of proteins, lipids, and inorganic compounds can be analyzed using FTIR spectroscopy [51, 55]. FTIR studies on cartilage have been carried out by several groups. The first IR studies to identify the primary components of cartilage were carried out by Camacho et al [51] . It was found that the infrared absorbances can show the variations in primary molecular components such as collagen and proteoglycan that reflected the quantity of components and distribution in the superficial, middle and deep zones. Typical spectra of the primary components of cartilage, collagen and the proteoglycan aggrecan, are shown in Figure 4.

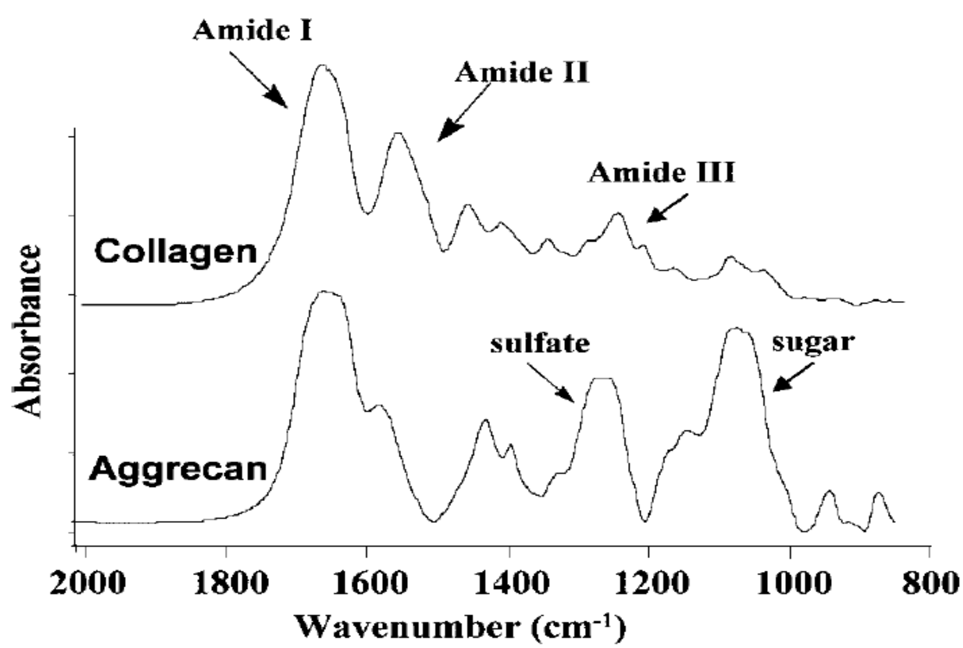

Figure 4 : Primary absorbances of collagen and aggrecan in cartilage

The amide I absorbance in the 1590-1720 cm^{-1} region arises from the C=O stretch of proteins, and the 958-1144 cm^{-1} absorbance arises from the sugar ring in PGs (Figure 5). The spectral parameter of 1326-1360cm^{-1} (centered at 1338cm^{-1}) was found to be an indicator of degenerated cartilage as the absorbance band decreased with collagen denaturation [49, 51]. This absorbance, when ratioed to an amide collagen absorbance, is referred to as "collagen integrity".

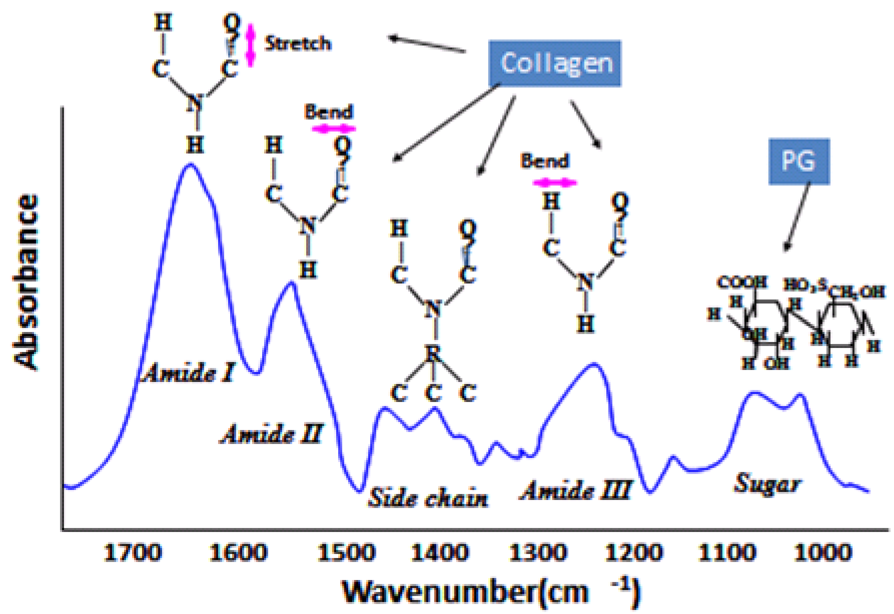

Figure 5 : Spectrum of primary absorbances in cartilage.

It has been shown that the amide I peak arises primarily from the C = O stretching vibration of type II collagen and possesses a transition moment oriented perpendicularly to the collagen fibril long axis [56]. The amide I and amide II modes have the transition moments that extend in perpendicular directions. Hence the structural orientation of collagen molecules can be assessed by the ratio of the collagen amide I/ amide II when a wire grid polarizer is inserted in between the sample and infrared beam, [57]. FTIR studies from research groups have shown that the collagen and proteoglycan content of the tissues correlated well with the histological determination of proteoglycan and the glycosaminoglycan derived from biochemical measurement [50, 58]. Studies have also shown correlations with magnetic resonance imaging studies [58, 59] . Thus together, these data demonstrate that FT-IRIS can be utilized to assess molecular and structural properties of cartilage.

CHAPTER 2: HYPOTHESIS AND SPECIFIC AIMS

The overall goal of this project is to find molecular indicators using Fourier transform infrared parameters alone or in conjunction with histological and immunohistochemical measurements to evaluate the quality of cartilage repair tissue in a rabbit osteochondral defect model.

Hypothesis 1: We hypothesized that FTIR spectroscopy is sensitive to the detection of molecular and compositional changes in articular cartilage repair tissue, and that infrared spectral imaging-derived parameters obtained from cartilage repair tissue in a rabbit osteochondral defect model will improve over time.

Aim 1: To perform quantitative assessments of FT-IRIS parameters in normal and repair tissue including collagen content, proteoglycan, collagen integrity and orientation of collagen fibers. The FT-IRIS data assessed from the repair tissue will be statistically compared to the data from the adjacent normal articular cartilage to evaluate whether the repair tissue parameters become more similar to normal cartilage parameters over time. Histology and immunohistochemistry assessments for proteoglycan content, and for distribution of type I and type II collagen, will also be carried out.

Aim 2: To correlate the infrared spectral parameters statistically with histological and immunohistochemical parameters of repair tissue. The ultimate goal is to assess which infrared parameters better predict either the histological score or the amount of type II collagen in the cartilage repair tissue. Together these data will contribute to a thorough analysis of cartilage repair tissue by infrared spectral analysis, and will form the basis for development of an infrared-based tissue score to be used as a clinical tool.

CHAPTER 3: MATERIALS AND METHODS

Animal Model

(The procedure described in this paragraph was previously carried out at Hospital for Special Surgery, New York, NY**):**

Bilateral full thickness osteochondral defects 3mm in diameter, 2.5 mm deep,were created by drilling down into the subchondral plate in mature New Zealand white rabbits. Animals were sacrificed using barbiturate overdose. The defect and surrounding tissues were removed and harvested at 2, 4, 6, 8, 12, and 16 weeks post-defect creation.

Tissue Preparation:

Immediately after harvesting the tissues were fixed in formalin, decalcified, and infiltrated by an automated infiltration processor and paraffin embedded for processing for infrared imaging, histology and immunohistochemistry. Tissues were sectioned at 7 µm thickness for infrared imaging and mounted onto low-e slides (Kevley Technologies, Chesterland, OH). Tissues were sectioned at 6 µm thickness for histological and immunohistochemical staining and mounted onto plus slides (~n = 5 per group). Imaging sections on the low-e slides were deparaffinized with xylene and 100 % ethanol and left air dried. The choice of tissue section thickness depends on the material and the purpose of the investigation. For histochemical studies that require more cellular details, and 3 – 6 µm thickness is preferred [60]. This range of thickness can provide a rich stain that is easier to interpret especially at 2X and 4X magnifications. For infrared imaging, the maximum penetration depth in the mid-IR (~400 – 4000 cm^{-1}) is up to 10 µ. The optimal thickness for infrared imaging will result in an absorbance close to or less than 1 (~ 10% of the radiation is transmitted), but not too low such that the spectra are noisy. The seven micron sections used in this study resulted in individual spectra with absorbances less than 1 that had a high signal to noise ratio.

Histological Grading:

Histological sections were deparaffinized with xylene and a series of ethanol grades (100, 95, 70 and 50) before staining. Sections were then stained with Hematoxylin and Eosin (H&E) and with Alcian blue for morphological and glycosaminoglycan (GAG) assessments. The histological sections from each specimen were examined and scored by two blinded independent observers using modified the O'Driscoll semi quantitative scoring system [43]. The following parameters were analyzed:

Nature of the predominant tissue:

The nature of the predominant tissue was defined as the tissue that was estimated histologically to comprise more than 50 percent of the total tissue in the defect. The predominant tissue was classified as (1) fibrous tissue, (2) poorly differentiated mesenchyme or (3) hyaline-like cartilage

The tissue can be considered as fibrous if it consists of spindle-shaped cells and the cells are closely associated with the surrounding collagenous matrix, and do not reside in lacunae. The matrix contains type I collagen fibers oriented parallel to each other which form bundles that lie roughly parallel to the surface. The collagen fibers are clearly visible at low power under polarized light and the matrix does not stain positively for GAGs. Fibrocartilage tissues are considered as an intermediate stage between those of fibrous tissue and hyaline cartilage. Cells are rounded and reside in lacunae surrounded by a pericellular matrix thus distinguishing fibro cartilage from fibrous tissue.

Hyaline cartilage is identified primarily by the characteristic appearance of its type II collagen matrix. Cells display a spherical morphology except near the surface where they are usually elongated as in normal articular cartilage. The cells reside in a well define lacunae. The matrix stains positively for glycosaminoglycan's with alcian blue staining.

Surface regularity:

Surface regularity was considered as grade (1) completely disrupted if there was severe fibrillation and fissuring (2) partially disrupted if there were minor fissures or slight amounts of fibrillation (3) smooth and intact if there were no fissures or fibrillation.

Structural integrity:

The structural integrity of the newly formed tissue was considered separately from the surface regularity. Structural Integrity refers to the degree to which the tissue below the surface appeared to be intact histologically [42]. The tissue was graded as 1 if it's completely disrupted with large horizontal clefts within the newly formed tissue or between it and the underlying subchondral bone. A grade of 2 represents partially disruption, if minor cleavage planes were observed or if fissures extended from the surface to the subchondral bone. A grade of 3 represents the tissue is smooth and intact.

Freedom from cellular changes of degeneration:

Freedom from cellular changes of degeneration was also considered. It consists of hypo cellularity and chondrocyte clustering. Freedoms from degenerative changes in adjacent cartilage were assessed as 1, if the tissue has normal cellularity, no clusters, and normal staining. Graded as 2 if it has normal cellularity, mild clusters, and moderate staining. 3, as mild or moderate hypo cellularity, slight staining and 0, as severe hypo cellularity, poor or no staining [42].

Bonding to the adjacent cartilage:

The newly formed tissue was considered to have a grade of 1, if there is no bonding at both ends of the defect to the adjacent cartilage. 2, if there is a partial bonding at one end of the defect to the adjacent cartilage or 3, if it's completely bonded at both ends to the adjacent cartilage. The graded histological scores were averaged from the two independent observers and the Mean ± SEM were plotted (Figure 7).

Immunohistochemical Staining

Immunohistochemical studies were carried out with the use of monoclonal antibodies against type I and type II collagen on the tissue sections that consisted of adjacent normal and repair tissue. Tissue sections were deparaffinized and rehydrated with xylene and a series of ethanol concentrations as described above. The sections were then treated either with an antigen retrieval for (collagen-I) or with a hyaluronidase digestion for (collagen – II) to unmask the collagen antigens. After a through wash with a PBS solution (1X) slides were then incubated with 0.5% Triton in PBS at room temperature for permeabilization. Endogenous peroxidase was blocked with 0.3% hydrogen peroxidase in methanol for 5 minutes at room temperature. After washing with PBS solution, the tissues were blocked in 4% bovine serum albumin (BSA) with 0.1% Tween20 for one hour at room temperature. After washing with PBS solution, mouse monoclonal primary antibody against type I collagen (Abcam Inc. Cambridge, MA) and rat monoclonal primary antibody against type II collagen (generously provided by Dr. Charlene Willams, Jefferson University, Philadelphia, PA) was diluted with 1% BSA with 0.1% Tween20 in 1:100 ratio and applied to all sections. It was allowed to incubate overnight at 4°C. Slides were washed with PBS and the secondary biotinylated antibodies against type I and type II collagen were applied and the slides were then incubated for 1 hour at room temperature. Following secondary antibody application the slides were incubated at room temperature for 30 minutes with horseradish peroxidase kit (Vector Laboratories Burlingame, CA). Washed with PBS again the slides were incubated at 37°C approximately for 20-30 minutes with DAB solution peroxidase substrate kit (Vector Laboratories), checking microscopically for the staining. Slides were dehydrated with 70, 95 and 100 % Ethanol, and cover slipped with Permount (Fischer)

Image Analysis and Quantification of Collagens:

Tissue sections were photographed with an Olympus MVX10 microscope (Olympus Optical Co. Ltd., Center Valley, PA) along with an Olympus DP70 camera at 2X magnification. The staining intensity was quantified using a programmed macro. To make our data consistent with infrared imaging data, a rectangular region of interest was selected for both normal and repair tissue. The staining intensity in the total region and the selected region were calculated with the macro. The values acquired represent the average pixel intensity within the region selected as well as the total region for both normal and repair tissues. The intensity values were normalized by the selected region of interest to the total region within each tissue type. Then the normalized intensity values were averaged by groups. The amount of type I and type II collagen from immunohistochemical experiments were normalized initially to the smallest value within the tissue type and then further normalized as follows: the defect region value normalized to the normal full thickness cartilage tissue, so as to see the percentage of type II collagen in the repair tissue.

FT-IRIS Data Acquisition:

FT-IRIS was performed using a Perkin Elmer Spectrum Spotlight 400 imaging spectrometer (Perkin Elmer, Shelton, CT). Infrared experiments were carried out in imaging mode with reflection optics. The background was recorded every time. A rectangular region of interest that contained the defect and adjacent normal cartilage was selected and data were acquired in the 4000 to 700 cm^{-1} spectral region at a spatial resolution of 25μm and spectral resolution of 8 cm^{-1}. For every sample, a polarized experiment was done by inserting a wire grid polarizer angled at 0°. Imaging data for repair and normal cartilage were analyzed using ISys 5.0 software (Malvern, UK).

Infrared Imaging Analysis:

The spectral region from ~900 – 2000 cm^{-1} was considered as it has been shown to contain molecular information that arises from collagen and proteoglycan, the primary components of cartilage [51]. Images were masked to three different regions as normal, adjacent normal and the repair tissue based on proteoglycan content. Considering the pathology of cartilage defects, the defect tissue is shown to have less proteoglycan in the this region compared to normal. Tissues were also masked based on their orientation considering the zonal distribution of cartilage parallel fibrils on the surface and random fibrils in the mid zone and perpendicular fibrils in the deep zone. Overall, the defect region was differentiated based on its surface features, the proteoglycan content and the collagen orientation. The region just next to the repair tissue and close to normal tissue was considered as the adjacent normal region.

Specific spectral absorbance bands arising from collagen, proteoglycan, collagen integrity, and orientation were evaluated [49]. Collagen and proteoglycan content were monitored by the integrated area of the peaks centered at 1660 and 1050 cm^{-1} absorbance's respectively. Collagen helical integrity was monitored by the ratio of the integrated area of the 1338 cm^{-1} collagen side chain absorbance to the amide II absorbance centered at 1550 cm^{-1}. Polarization experiments were also performed to determine the distribution of the collagen fibril orientation by assessment of the ratio of the collagen amide I/amide II absorbance. Ratio's were masked to the range of 1-4 where a ratio $\geq$ 2.7 reflects, fibrils aligned parallel to the articular surface, ratio $\leq$ 1.7 reflects fibrils perpendicular to the articular surface and ratio between 2.7-1.7, reflects a random fibril orientation [57] (Figure 6G). The percentage of collage fibril orientation was assessed quantitatively as follows: Pixels associated with the polarized FT-IRIS images were divided into the three orientation categories as described above and the percentage falling into each category were calculated.

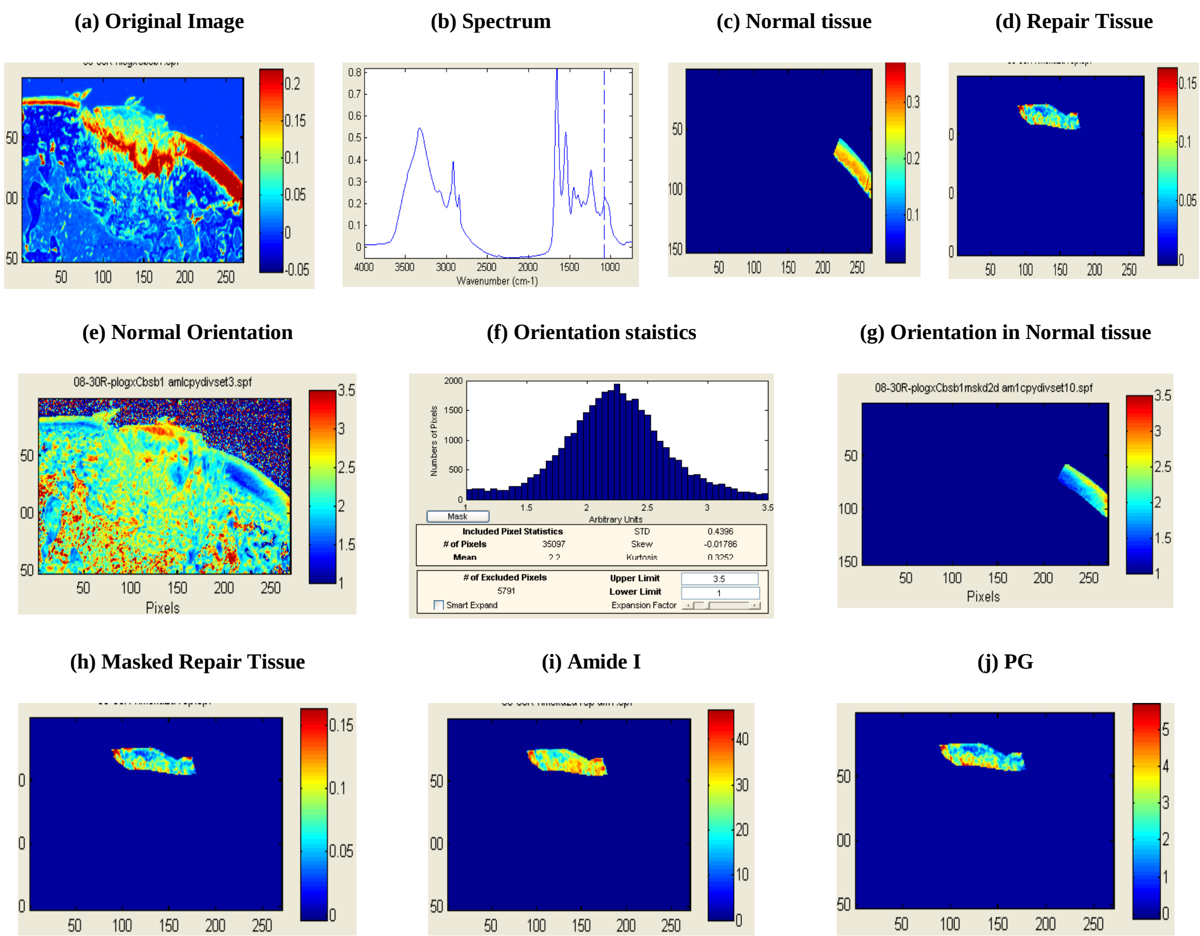

(k) PG / Am I **(l) Collagen Integrity(1338/Am II)** **(m) Orientation**

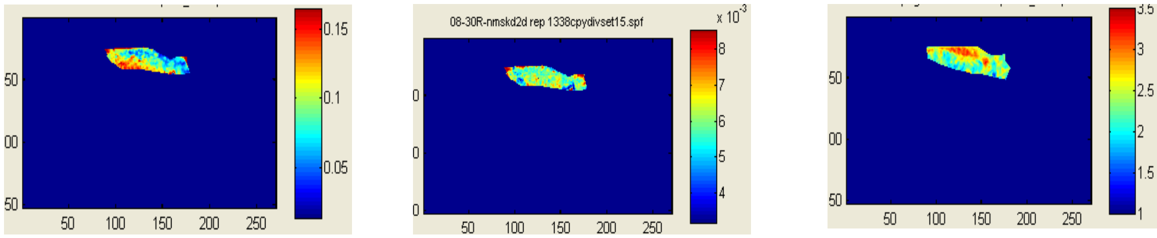

Figure 6 : Infrared imaging spectral parameters in repair tissue. Original image based on proteoglycan content shown in (a), typical spectrum shown in (b) masking of normal tissue PG content and orientation shown in (c) and (g); masking of different parameters of repair tissue shown in (d), and in (h-m). Orientation of entire tissue and pixel distribution of orientation values shown in (E) and (F), respectively.

CHAPTER 4: STATISTICAL METHODS

The integrated areas of the infrared absorbances were calculated for normal and the repair tissues for the following parameters: collagen and proteoglycan content, collagen integrity, the proteoglycan absorbance ratio to amide I. Results were plotted as Mean ± SEM. A paired Student's t test was used to compare the normal and repair values within each group. The significance of differences among all six groups was determined by one-way Analysis of Variance (ANOVA, SigmaStat 3.1, Systat Software Inc., San Jose, CA) followed by a Tukey's test for post hoc group by group comparison with an overall p value < 0.05 considered significant. All the parameters were separately correlated with histological scores, and with quantitative analysis of type I and type II collagen from immunohistochemical analysis.

In order to further investigate which infrared parameter would better predict the histological grade or am amount of type II collagen, a multiple linear regression technique was used.

The following regression models were derived by considering infrared parameters as the independent variables and the histological grade and type II collagen as dependent variables. All infrared parameters were normalized for the analysis.

a. Prediction of histological scores with amide I, proteoglycan content, and collagen helical integrity in the repair tissue.

b. Prediction of histological scores with proteoglycan ratio to amide I and collagen integrity.

c. Prediction of histological scores with proteoglycan and collagen integrity.

d. Prediction of of type II collagen content with amide I, proteoglycan content and the collagen integrity.

e. Prediction of type II collagen content with proteoglycan and collagen integrity.

f. Prediction of type II collagen with PG/AM1 and Collagen integrity.

CHAPTER 5: RESULTS

Histological results:

There was an overall improvement in the fill of the defect and quality of the tissue over time as shown from the histological scores, and qualitatively in the images (Figures 7,8). There was a general trend towards increasing histological score from two to 16 weeks, except for the 12th week. A significant difference between weeks 2 and 16, and 8 and 16, was observed by one way ANOVA.

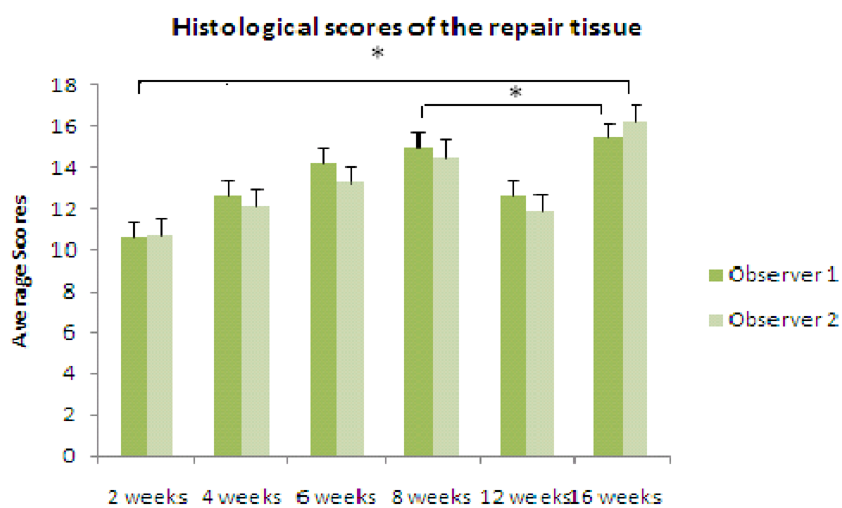

Figure 7 : Histological score averaged per group (~ n = 5) graded by two independent observers * p < 0.05.

The inter-observer agreement between the observers was calculated by a kappa calculator. The overall kappa statistic value was 0.81, which qualifies as almost perfect as stated by Landis et al, [61]

The nature of the predominant tissue was hyaline in only ~12% of all the samples (3/25), and ~60% of the samples were healed with fibrocartilage. The surface regularity was smooth and intact in 24% of the samples. Approximately 12% of the 16 week samples have a normal proteoglycan staining and 57% of the samples were bonded to the adjacent cartilage at both ends.

Immunohistochemistry:

Immunohistochemistry results demonstrated immunostaining for type I collagen in some samples and type II collagen in most samples (Figure 8). The positive type I collagen is attributable to the fibrous tissue that was formed initially. Normal articular cartilage was immunopositive for type II collagen with almost no staining for type I collagen. As expected, the highest area of immunostaining for type I collagen was seen in fibrous tissue at earlier timepoints, and less in cartilage repair tissue at later timepoints, especially in 12 and 16 week samples. Some of the 8 week samples stained with type II collagen and some type I collagen. The percentage of areas of sections with type I collagen staining was at a minimum in 12 week repair tissues, although this group did not have the correspondingly highest histological grade .

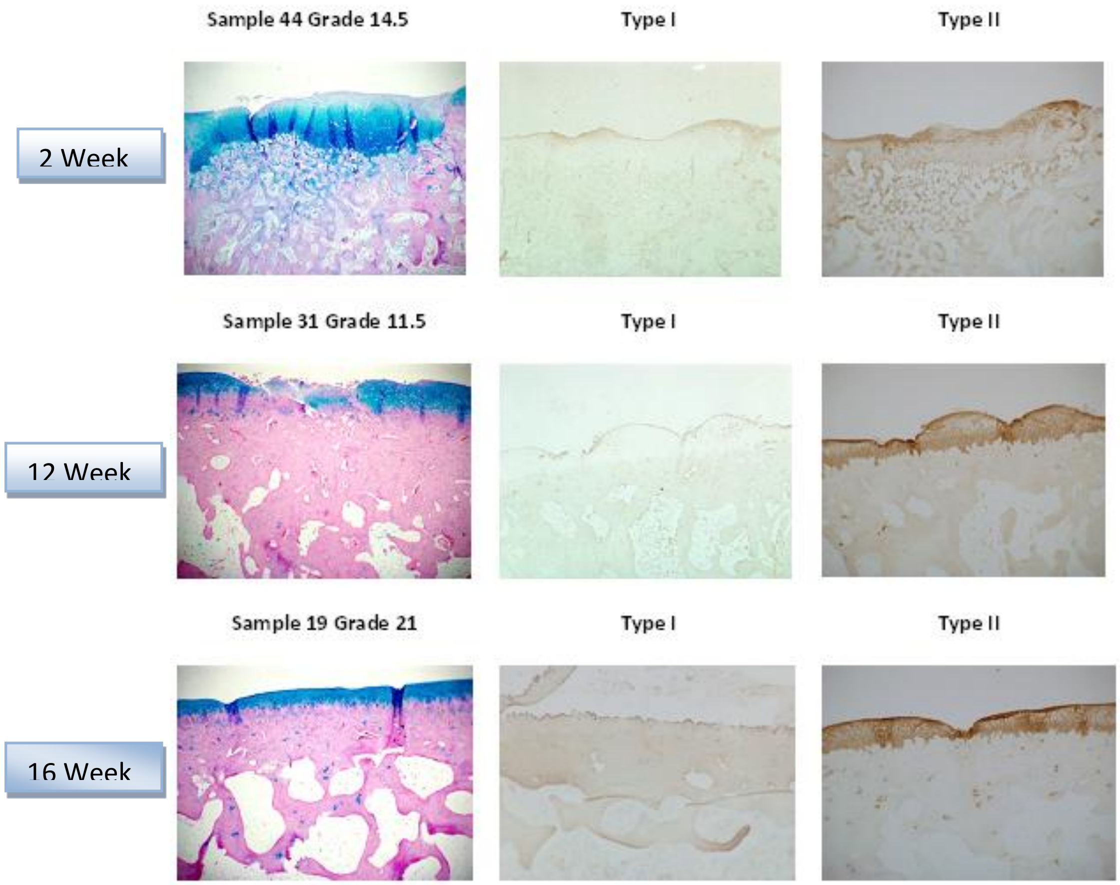

Figure 8 : Progression in repair tissue quality, histological grade and its corresponding amount of type I and type II collagen staining at 2, 12 and 16 weeks repair.

Infrared imaging results:

Quantitative data show that compared to adjacent normal cartilage, the repair tissue had a lower collagen and collagen integrity in the initial weeks but reached values comparable to normal tissue by 8 weeks (Figure 9). PG content did not reach the levels found in the normal articular cartilage. Based on histological scores and IR parameters, it was also evident that the defect region was filled with repair tissue at 8 weeks in most of the samples. As expected, most of the samples have demonstrated higher contents of collagen, proteoglycan and collagen integrity in adjacent normal articular cartilage compared to repair tissue.

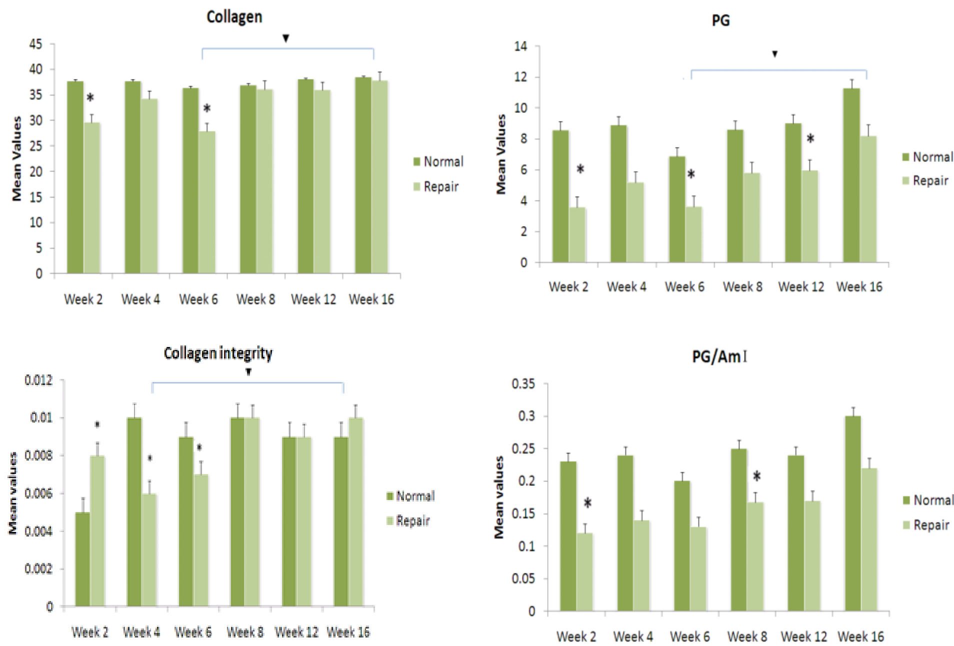

Figure 9 : FTIR parameters of collagen, proteoglycan, collagen integrity and PG/AmI. Averages per group were plotted (~n=5means with SEM, and). Significant differences at p <0.05 were shown with ▼ for repair tissue at different time points, and with a * between repair and normal tissue at the same timepoint.

From the ANOVA results, significant differences were observed in repair tissue from 6 weeks to the16 week timepoints in collagen and proteoglycan content, indicating a significant improvement from starting at 6 weeks in most of the samples. A similar improvement was found for collagen integrity, comparing the observed values between 4 and 16 weeks, whereas the collagen fibril orientations had no statistical difference throughout the 16 week period (Figure 10).

There was no zonal stratification of collagen fibril orientation as seen in normal articular cartilage throughout the 16 weeks of the study, and in particular, a lower amount of fibrils perpendicular to the articular surface. Differences in these parameters in the repair tissue compared to the normal tissue likely reflect the presence of fibrocartilage.

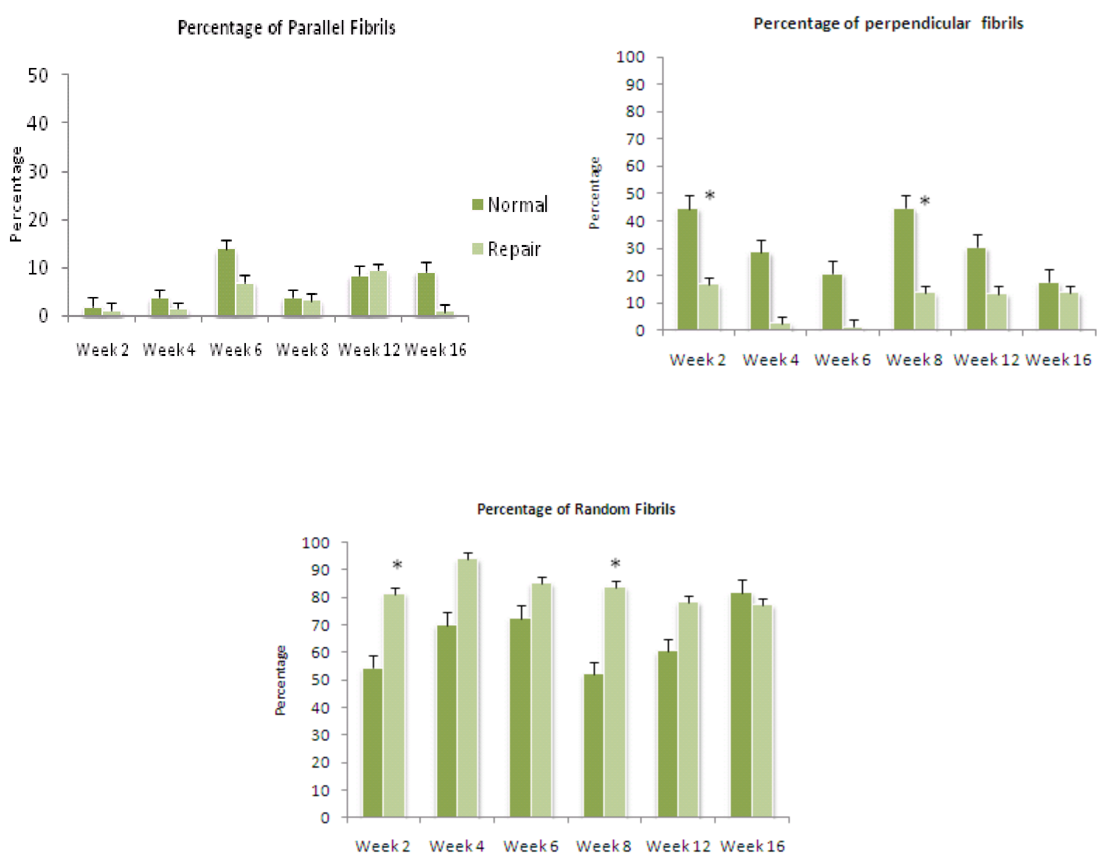

Figure 10 : Percentage of collagen fibrillar orientation averages per group with SEM (n ~ 5) * p < 0.05 comparison of repair tissue vs normal at each timepoint.

Correlations

Further investigations were done to assess the individual parameters of the three different outcome measures and to determine which infrared parameters would have a good correlation with either the immunohistochemistry or the histology results, Accordingly, IR parameters were compared to type II collagen staining, overall histological grade, nature of predominant tissue (amount of hyaline cartilage present), structural integrity, and to the grade of proteoglycan staining. These features were chosen for comparison, as they represent the desired outcomes for cartilage repair.

The correlation of the grade of the nature of the predominant tissue and the proteoglycan content derived infrared spectral parameter gave an R^2 of 90%, and the correlation of proteoglycan staining score and infrared-derived proteoglycan content resulted in an R^2 of 74%. The correlation of histological grade of structural integrity and the collagen integrity (ratio of 1338/Am II) gave an R^2 of 79%. These correlations were significant at the $P < 0.05$ level, and together, these data indicate that FTIR is highly sensitive to the structural and molecular changes that occur during the repair process.

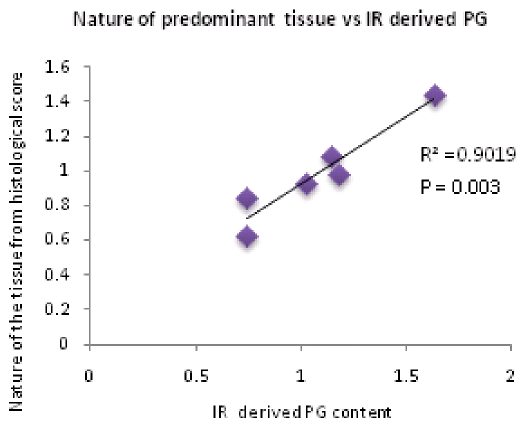
Nature of predominant tissue vs IR derived PG
Nature of the tissue from histological score
IR derived PG content
R^2 =0.9019
P = 0.003
1.6
1.4
1.2
1
0.8
0.6
0.4
0.2
0
0
0.5
1
1.5
2

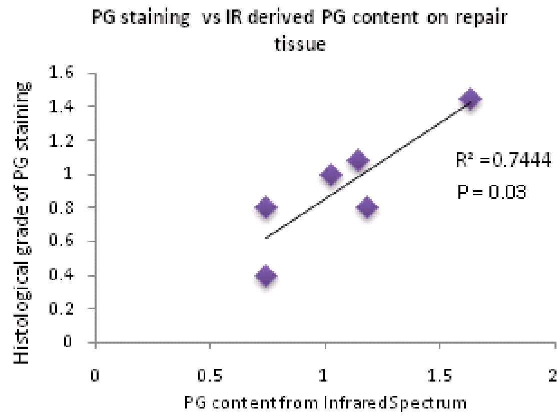
PG staining vs IR derived PG content on repair tissue
Histological grade of PG staining
PG content from Infrared Spectrum
R^2 =0.7444
P = 0.03
1.6
1.4
1.2
1
0.8
0.6
0.4
0.2
0
0
0.5
1
1.5
2

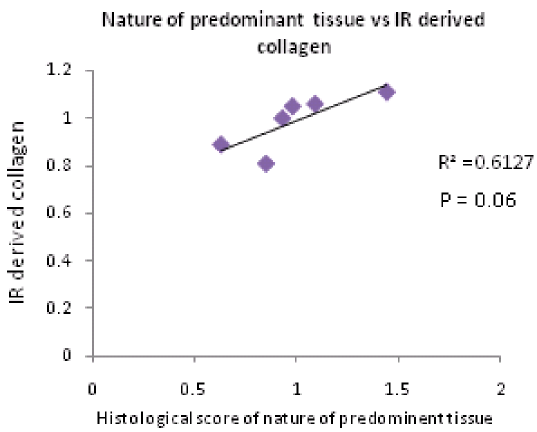
Nature of predominant tissue vs IR derived collagen
IR derived collagen
Histological score of nature of predominent tissue
R^2 =0.6127
P = 0.06
1.2
1
0.8
0.6
0.4
0.2
0
0
0.5
1
1.5
2

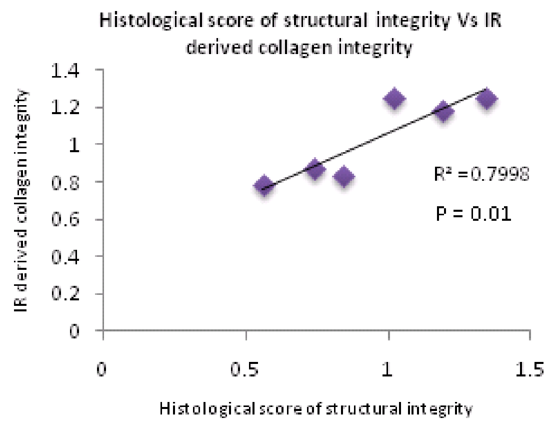
Histological score of structural integrity Vs IR derived collagen integrity
IR derived collagen integrity
Histological score of structural integrity
R^2 =0.7998
P = 0.01
1.4
1.2
1
0.8
0.6
0.4
0.2
0
0
0.5
1
1.5

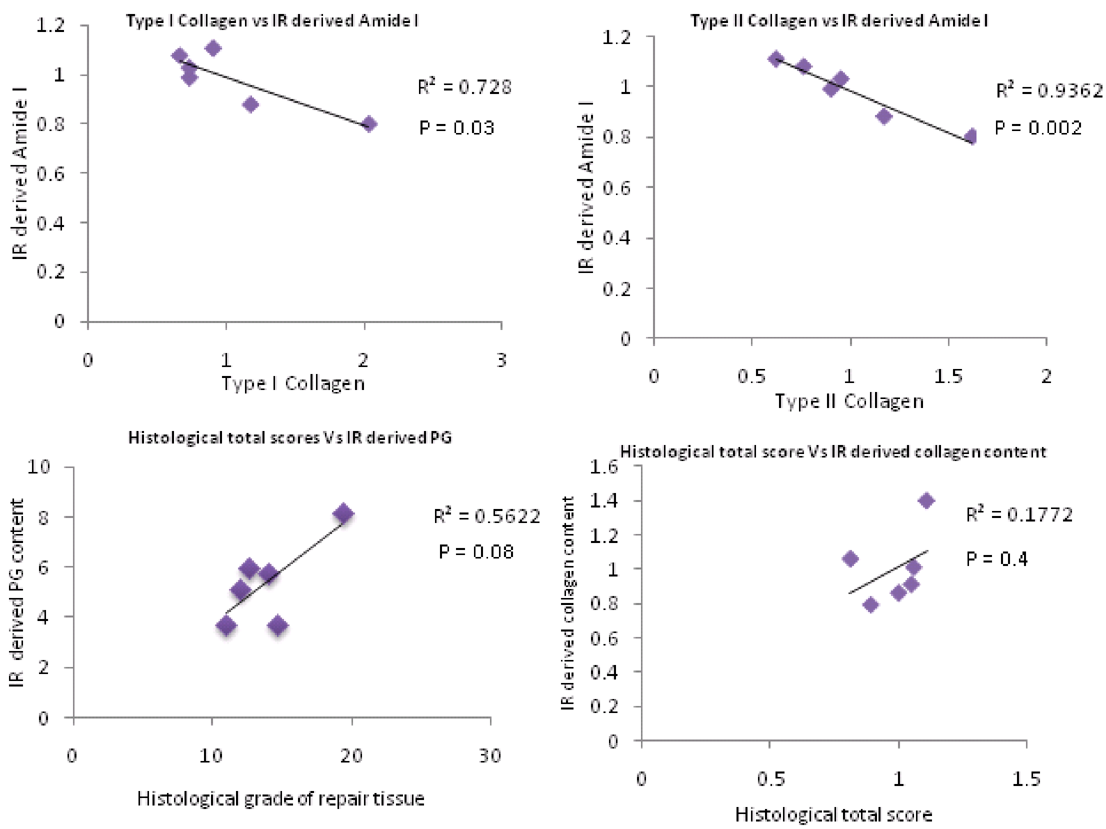

Figure 11 : Correlations of IR derived parameters to histological grade and type I and type II collagen based on group average values. a) Nature of the predominant tissue grade vs IR derived PG b) Proteoglycan staining grade vs IR derived PG c) Nature of the predominant tissue grade vs IR derived collagen d) Structural integrity grade vs IR derived collagen integrity e) Staining intensities of type II collagen with IR derived collagen content (amide I) f) Type I collagen staining vs IR derived collagen. g) Histological total score vs IR derived PG h) Histological total score vs IR derived collagen content. Correlations were significant at the p < 0.05 level, except for the total histological grade vs IR derived PG and collagen, and nature of predominant tissue vs IR derived amide I

Regression Analysis

Multiple linear regression analysis was performed, on normalized values to assess whether a combination of several infrared-derived parameters would correlate to the histological score and amount of type II collagen better than a single parameter.

- Regression equations were derived by considering the collagen, proteoglycan content and the collagen integrity, and PG/Am I of the repair tissue as independent variables to predict the final histological grade**.**

  With Amide I, PG, and collagen integrity:

  *Histological Grade = 30.670 - (1.130 * Amide I) + (3.236 * PG) + (476.952 * collagen integrity (R^2 = 0.956)*

  With PG/Am I, collagen integrity:

  *Histological Grade = 3.377 + (71.352 * Pg/am1) - (78.810 * collagen integrity) (R^2= 68)*

  With PG and collagen integrity:

  *Histological Grade = 5.768 + (1.069 * PG) + (294.948 * collagen integrity) (R^2=57.6)*

  From these equations, it is evident that the collagen integrity has the highest impact in predicting the grade with a high correlation.

- Regression equations were also derived considering the above mentioned IR parameters to predict the amount of type II collagen in the repair tissue

Type II collagen with amide I, PG and collagen integrity

*Type II collagen = 7.072 - (0.197 * Amide I) + (0.0809 * PG) + (85.522 * Collagen integrity) (R^2= 68)*

Type II collagen with collagen integrity and PG/Am I

*Type II collagen = 3.115 + (17.381 * Collagen integrity) - (10.760 * PG/Am I) (R^2= 42.9)*

Type II collagen with PG, and Collagen integrity:

*Type II collagen = 2.743 - (0.296 * PG) + (53.880 * Collagen integrity) (R^2= 0.571)*

Similar to the regression model to predict histological grade, the use of the three infrared infrared parameters together that reflect collagen, PG, and collagen integrity, gave the best prediction of type II collagen content.

CHEPTER 6: DISCUSSION

This study provides an extensive analysis of Fourier transform infrared spectral parameters in conjunction with the standard histological and immunohistochemical assessments. Quantitative histological methods were used for the evaluation of the repair tissue in defects. For a preliminary investigation of healing, histology provides the widest range of information which is widely accepted and is considered the standard to which other modalities utilized to evaluate repair tissue are compared. Here we studied the usage of FTIR imaging of repair cartilage and evaluated the repair process, compared and correlated it to the standard histological assessments. The use of several IR parameters together correlated very well with histological grade, supporting these use of these parameters as an "infrared score" to evaluate molecular and compositional structure of cartilage. The use of infrared fiber optic methodology could enable the molecular structure of the chondral surface to be conveniently evaluated using currently available arthroscopic techniques. Thus, these data also support the long term goal of this project, to develop an accurate method to evaluate repair tissue quality, and thereby extending the usage of mid infrared fiber optic probe to a clinical setting as a diagnostic tool to evaluate repair tissue in arthroscopic procedures.

The Fourier transform infrared imaging analysis studies performed permit evaluation of the primary structural and molecular changes that occur in repair tissue. Previously other FT-IRIS studies were carried out, including monitoring enzymatic collagenase degradation [62], assessment of collagen fibril orientation in cartilage [57], evaluation of proteoglycan in tissue engineered cartilage [50] evaluation of human osteoarthritic cartilage [59, 63] and rabbit repair tissue after treatment with a therapeutic peptide [58]. Although the study by Kim et al [58] assessed collagen, collagen integrity and proteoglycan content correlations with magnetic resonance imaging, they only compared two time points, and thus a thorough comparison of cartilage repair tissue and native cartilage by infrared spectral analysis in a long term study has not been done until now. Here in this study, we carried out an infrared spectral analysis of repair tissue and native cartilage combining with standard outcome measures to find molecular indicators of repair tissue progress.

In this study we have observed an improvement by morphological and infrared analysis throughout the 16 week period. These results are in agreement with the natural history of fibrocartilaginous healing in untreated defects [36, 64, 65]. However, it is interesting to note that there was much variability in healing response as some samples had demonstrated an incomplete healing, while some others have an excessive healing of the defect within a group. Factors that underlie the variability in healing are not known for sure, but it is possible that a result of the variable healing could be differences in cellularity of the tissue. In general, fibro cartilage is less cellular than hyaline cartilage, the cellular characteristics in reparative fibrocartilage are smaller and irregularly arranged [66]. The healing of the defect in general becomes filled with loose fibro vascular network that gradually becomes more cellular and less vascular [67]. If this is the case, a higher cellularity in the tissue could also interfere with the accuracy of the infrared spectral results. The presence of increased cellularity could complicate assessment of matrix components, by having too large a contribution from the cells that would essentially dilute the contribution of the collagen or PG to the infrared spectra. Further, previous studies that investigated cellular spectra have found that the observed spectra of the cells and tissues are not always a linear combination of basis spectra. These studies have observed that the protein spectra undergo quite significant changes that may be positively or negatively correlated to the changes in cellular components [68, 69], and have reported significant shifts in amide I and II frequencies in cellular effects or diseased states.

Another possible factor that would affect the infrared spectral parameters is tissue section thickness, as the individual absorbance peaks in any infrared spectrum could vary according to thickness. According to [70], especially for histochemical studies, even though a consistent section thickness is followed for all the sections, the assumption that consecutive sections are of the same thickness at any given microtome setting is not strictly true.

The immunohistochemical analysis has shown that the presence of type II collagen was less in repair tissue, which also had fibrocartilage morphology from the histological point of view. The presence of type I collagen was observed in fibrous tissue as expected. From the correlations shown in this study it was also observed that there was a strong negative correlation between the type I and type II collagen and IR-derived collagen content. The differences in the cellularity as stated earlier possibly interfere with the spectra, as Diem et al [68] stated in an earlier work, that the spectra undergo significant changes with the presence of a protein, and may result in negative correlation. However the negative correlation of amide I in repair tissue needs to be further investigated.

Our infrared analysis has consistently shown a progress in repair throughout the 16 weeks of study, even though proteoglycan content never reached the values of normal articular cartilage, and there was no orientation of collagen fibrils. In spite of this, the correlation of the nature of the predominant tissue to IR-determined proteoglycan and collagen content was a very encouraging result, with significant correlation coefficients, but PG correlation greater than that for collagen. This shows that the level of proteoglycan, whether determined histologically or by IR, can be a determinant for the type of cartilage (hyaline or fibro) present in the tissue. The reason behind a slightly low correlation factor for amide I region may be that while amide I has been proven to correlate with the amount of collagen [49, 51] , there are other factors besides collagen content that makeup the hyaline nature of the tissue.

The collagen integrity and the histological grade of structural integrity also resulted in a significant correlation, with an R^2 value of 79%. From the regression analysis, it was observed that the collagen integrity has the highest impact on histological score. From the regression analysis, to predict the amount of type II collagen with different PG, PG/Am1, collagen integrity and amide I parameters, it is again the collagen integrity that has a high coefficient and a good correlation. From these results, it is clear that the histological grade of the repair tissue can be predicted with collagen integrity. Although previous studies [71], have shown that the collagen integrity (1338 ratio to amide II) decreased with collagen degeneration, this is the first study to show that it also positively correlates with cartilage repair, eg, the synthesis of new collagen.

In summary, FT-IR evaluation has been shown to be an effective measure of cartilage histological tissue grade and collagen type. Given the possibility of using this in a fiber optic format, where sampling of the intact chondral surface is possible [63] it may be possible to monitor the efficacy of new treatment methods in cartilage defects. However, in spite of the advantages that FT-IR offers, there are certain limitations to this technique. The invasiveness and the need to harvest the tissue for imaging studies remain as the main limitations to this technique. Further, histological sections are completely dehydrated during the deparaffinization process as they have to undergo a series of decreasing grades of ethanol's, and typically the only water that remains in the tissue is structural water. Thus, the correlations defined here were to dehydrated tissues. The alternative for this limitation is the infrared fiber optic probe designed to be used arthroscopically [59], but it is likely that evaluation of hydrated cartilage samples will require additional data evaluations to account for the contribution of water.

The histochemical and imaging analysis results suggest that Fourier transform infrared imaging spectroscopy is sensitive to the structural and molecular changes even in early stages. In the future, further investigations into these data may lead to the development of a new scoring that would utilize infrared spectral parameters alone to assess regenerated articular cartilage. As new cartilage treatment methods come into use, there will always be a requirement for quantitative evaluation of the regenerated tissue. A reliable method if established would assist in the solution of the important clinical questions, such as to determine if the repair tissue is progressing as desired, and the possibility to assess the tissue type if the regenerated cartilage as fibrous or a hyaline.

REFERENCES CITED

1. Alford JW, Cole BJ (2005) Cartilage Restoration, Part 1. The American Journal of Sports Medicine 33:295-306
2. Aigner T, Stöve J (2003) Collagens--major component of the physiological cartilage matrix, major target of cartilage degeneration, major tool in cartilage repair. Advanced Drug Delivery Reviews 55:1569-1593
3. Ulrich-Vinther M, Maloney MD, Schwarz EM, Rosier R, O'Keefe RJ (2003) Articular Cartilage Biology. J Am Acad Orthop Surg 11:421-430
4. Umlauf D, Frank S, Pap T, Bertrand J Cartilage biology, pathology, and repair. Cellular and Molecular Life Sciences 67:4197-4211
5. Poole AR, Kojima T, Yasuda T, Mwale F, Kobayashi M, Laverty S (2001) Composition and Structure of Articular Cartilage: A Template for Tissue Repair. Clinical Orthopaedics and Related Research 391:S26-S33
6. Glass GG (2006) Osteoarthritis. Disease-a-Month 52:343-362
7. Levesque MC (2007) Causes of osteoarthritis, Medicinenet. In:
8. Adkisson HD, Martin JA, Amendola RL, Milliman C, Mauch KA, Katwal AB, Seyedin M, Amendola A, Streeter PR, Buckwalter JA The Potential of Human Allogeneic Juvenile Chondrocytes for Restoration of Articular Cartilage. The American Journal of Sports Medicine 38:1324-1333
9. Alford JW, Cole BJ (2005) Cartilage Restoration, Part 2. The American Journal of Sports Medicine 33:443-460

10. Robinson D, Nevo Z (2001) Articular Cartilage Chondrocytes are more Advantageous for Generating Hyaline-like Cartilage than Mesenchymal Cells Isolated from Microfracture Repairs. Cell and Tissue Banking 2:23-30
11. Yannas IV, Kinner B, Capito RM, Spector M (2005) Regeneration of Articular Cartilage. In: Regenerative Medicine II. Springer Berlin / Heidelberg, p 129-130
12. Anderson AF, Smith M (2009) Progress in Cartilage Restoration. The American Journal of Sports Medicine 37:7S-9S
13. Roberts S, McCall I, Darby A, Menage J, Evans H, Harrison P, Richardson J (2003) Autologous chondrocyte implantation for cartilage repair: monitoring its success by magnetic resonance imaging and histology. Arthritis Res Ther 5:R60 - R73
14. Lorenz H, Richter W (2006) Osteoarthritis: Cellular and molecular changes in degenerating cartilage. Progress in Histochemistry and Cytochemistry 40:135-163
15. Murawski CD, Foo LF, Kennedy JG A Review of Arthroscopic Bone Marrow Stimulation Techniques of the Talus. Cartilage 1:137-144
16. Steinwachs MR, Th G, Kreuz PC (2008) Marrow stimulation techniques. Injury 39:26-31
17. Amiel D, Coutts RD, Abel M, Stewart W, Harwood F, Akeson WH (1985) Rib perichondrial grafts for the repair of full-thickness articular-cartilage defects. A morphological and biochemical study in rabbits. J Bone Joint Surg Am 67:911-920

18. Brittberg M, Sjögren-Jansson E, Lindahl A, Peterson L (1997) Influence of fibrin sealant (Tisseel®) on osteochondral defect repair in the rabbit knee. Biomaterials 18:235-242

19. Fuller JAMBCB, Ghadially FNMDPDDSCMRCP Ultrastructural Observations on Surgically Produced Partial-thickness Defects in Articular Cartilage. SO - Clinical Orthopaedics & Related Research July/August 1972;86:193-205

20. Green WTJMD Articular Cartilage Repair: Behavior of Rabbit Chondrocytes During Tissue Culture and Subsequent Allografting. SO - Clinical Orthopaedics & Related Research May 1977;124:237-250

21. Rudert M (2002) Histological Evaluation of Osteochondral Defects: Consideration of Animal Models with Emphasis on the Rabbit, Experimental Setup, Follow-Up and Applied Methods. Cells Tissues Organs 171:229-240

22. Salter RB, Simmonds DF, Malcolm BW, Rumble EJ, MacMichael D, Clements ND (1980) The biological effect of continuous passive motion on the healing of full-thickness defects in articular cartilage. An experimental investigation in the rabbit. J Bone Joint Surg Am 62:1232-1251

23. Frenkel SR, Bradica G, Brekke JH, Goldman SM, Ieska K, Issack P, Bong MR, Tian H, Gokhale J, Coutts RD, Kronengold RT (2005) Regeneration of articular cartilage - Evaluation of osteochondral defect repair in the rabbit using multiphasic implants. Osteoarthritis and Cartilage 13:798-807

24. Saw K-Y, Hussin P, Loke S-C, Azam M, Chen H-C, Tay Y-G, Low S, Wallin K-L, Ragavanaidu K (2009) Articular Cartilage Regeneration With Autologous

Marrow Aspirate and Hyaluronic Acid: An Experimental Study in a Goat Model. Arthroscopy: The Journal of Arthroscopic & Related Surgery 25:1391-1400

25. van Susante JLC, Buma P, Schuman L, Homminga GN, van den Berg WB, Veth RPH (1999) Resurfacing potential of heterologous chondrocytes suspended in fibrin glue in large full-thickness defects of femoral articular cartilage: an experimental study in the goat. Biomaterials 20:1167-1175

26. Yan H, Yu C (2007) Repair of Full-Thickness Cartilage Defects With Cells of Different Origin in a Rabbit Model. Arthroscopy: The Journal of Arthroscopic & Related Surgery 23:178-187

27. Kandel RA, Grynpas M, Pilliar R, Lee J, Wang J, Waldman S, Zalzal P, Hurtig M (2006) Repair of osteochondral defects with biphasic cartilage-calcium polyphosphate constructs in a Sheep model. Biomaterials 27:4120-4131

28. Milano G, Sanna Passino E, Deriu L, Careddu G, Manunta L, Manunta A, Saccomanno MF, Fabbriciani C The effect of platelet rich plasma combined with microfractures on the treatment of chondral defects: an experimental study in a sheep model. Osteoarthritis and Cartilage 18:971-980

29. Breinan HAP, Hsu HPM, Spector MP (2001) Chondral Defects in Animal Models: Effects of Selected Repair Procedures in Canines. Clinical Orthopaedics & Related Research 391:S219-S230

30. Bail H, Klein P, Kolbeck S, Krummrey G, Weiler A, Schmidmaier G, Haas NP, Raschke MJ (2003) Systemic application of growth hormone enhances the early healing phase of osteochondral defects--a preliminary study in micropigs. Bone 32:457-467

31. Cui W, Wang Q, Chen G, Zhou S, Chang Q, Zuo Q, Ren K, Fan W Repair of articular cartilage defects with tissue-engineered osteochondral composites in pigs. Journal of Bioscience and Bioengineering In Press, Corrected Proof

32. Mussa R, Hans MG, Enlow D, Goldberg J (1999) Condylar cartilage response to continuous passive motion in adult guinea pigs: A pilot study. American Journal of Orthodontics and Dentofacial Orthopedics 115:360-367

33. Kamali F, Bayat M, Torkaman G, Ebrahimi E, Salavati M (2007) The therapeutic effect of low-level laser on repair of osteochondral defects in rabbit knee. Journal of Photochemistry and Photobiology B: Biology 88:11-15

34. Virén T, Saarakkala S, Jurvelin JS, Pulkkinen HJ, Tiitu V, Valonen P, Kiviranta I, Lammi MJ, Töyräs J Quantitative Evaluation of Spontaneously and Surgically Repaired Rabbit Articular Cartilage Using Intra-Articular Ultrasound Method in situ. Ultrasound in Medicine & Biology 36:833-839

35. Hunziker EB (2002) Articular cartilage repair: basic science and clinical progress. A review of the current status and prospects. Osteoarthritis and Cartilage 10:432-463

36. Brittberg M, Lindahl A, Nilsson A, Ohlsson C, Isaksson O, Peterson L (1994) Treatment of Deep Cartilage Defects in the Knee with Autologous Chondrocyte Transplantation. New England Journal of Medicine 331:889-895

37. Hyllested Jl Fau - Veje K, Veje K Fau - Ostergaard K, Ostergaard K Histochemical studies of the extracellular matrix of human articular cartilage--a review.

38. Ceuninck F, Sabatini M, Pastoureau P, Melrose J, Smith S, Ghosh P (2004) Histological and Immunohistological Studies on Cartilage. In: Walker JM (ed) Cartilage and Osteoarthritis. Humana Press, p 39-63

39. Rutgers M, van Pelt MJP, Dhert WJA, Creemers LB, Saris DBF Evaluation of histological scoring systems for tissue-engineered, repaired and osteoarthritic cartilage. Osteoarthritis and Cartilage 18:12-23

40. Grogan SP, Barbero A, Winkelmann V, Rieser F, Fitzsimmons JS, Oâ€™Driscoll S, Martin I, Mainil-Varlet P (2006) Visual Histological Grading System for the Evaluation of in Vitroâ€“Generated Neocartilage. Tissue Engineering 12:2141-2149

41. Moojen DJF, Saris DBF, Auw Yang KG, Dhert WJA, Verbout AJ (2002) The Correlation and Reproducibility of Histological Scoring Systems in Cartilage Repair. Tissue Engineering 8:627-634

42. O'Driscoll SW, Keeley FW, Salter RB (1986) The chondrogenic potential of free autogenous periosteal grafts for biological resurfacing of major full-thickness defects in joint surfaces under the influence of continuous passive motion. An experimental investigation in the rabbit. J Bone Joint Surg Am 68:1017-1035

43. O'Driscoll SW, Keeley FW, Salter RB (1988) Durability of regenerated articular cartilage produced by free autogenous periosteal grafts in major full-thickness defects in joint surfaces under the influence of continuous passive motion. A follow-up report at one year. J Bone Joint Surg Am 70:595-606

44. Mainil-Varlet P, Van Damme B, Nesic D, Knutsen G, Kandel R, Roberts S A New Histology Scoring System for the Assessment of the Quality of Human Cartilage Repair: ICRS II. The American Journal of Sports Medicine 38:880-890

45. Roberts S, Menage J, Sandell LJ, Evans EH, Richardson JB (2009) Immunohistochemical study of collagen types I and II and procollagen IIA in human cartilage repair tissue following autologous chondrocyte implantation. The Knee 16:398-404

46. Sellers RS, Zhang R, Glasson SS, Kim HD, Peluso D, D'Augusta DA, Beckwith K, Morris EA (2000) Repair of Articular Cartilage Defects One Year After Treatment with Recombinant Human Bone Morphogenetic Protein-2 (rhBMP-2). J Bone Joint Surg Am 82:151-160

47. Smith BC (1995) Fundamentals of fourier transform infrared spectroscopy.

48. Smith BC Fundamentals of Fourier Transform infrared Spectroscopy.

49. Boskey A, Pleshko Camacho N (2007) FT-IR imaging of native and tissue-engineered bone and cartilage. Biomaterials 28:2465-2478

50. Kim M, Bi X, Horton JWE, Spencer RG, Camacho NP (2005) Fourier transform infrared imaging spectroscopic analysis of tissue engineered cartilage: histologic and biochemical correlations. Journal of Biomedical Optics 10:031105-031106

51. Camacho NP, West P, Torzilli PA, Mendelsohn R (2001) FTIR microscopic imaging of collagen and proteoglycan in bovine cartilage. Biopolymers 62:1-8

52. Erukhimovitch V, Pavlov V, Talyshinsky M, Souprun Y, Huleihel M (2005) FTIR microscopy as a method for identification of bacterial and fungal infections. Journal of Pharmaceutical and Biomedical Analysis 37:1105-1108

53. Fernandez DC, Bhargava R, Hewitt SM, Levin IW (2005) Infrared spectroscopic imaging for histopathologic recognition. Nat Biotech 23:469-474

54. Petibois C, Desbat B Clinical application of FTIR imaging: new reasons for hope. Trends in Biotechnology 28:495-500

55. Camacho NP, West P, Griffith MH, Warren RF, Hidaka C (2001) FT-IR imaging spectroscopy of genetically modified bovine chondrocytes. Materials Science and Engineering: C 17:3-9

56. Gadaleta SJ, Landis WJ, Boskey AL, Mendelsohn R (1996) Polarized FT-IR Microscopy of Calcified Turkey Leg Tendon. Connective Tissue Research 34:203-211

57. Bi X, Li G, Doty SB, Camacho NP (2005) A novel method for determination of collagen orientation in cartilage by Fourier transform infrared imaging spectroscopy (FT-IRIS). Osteoarthritis and Cartilage 13:1050-1058

58. Kim M, Foo LF, Uggen C, Lyman S, Ryaby JT, Moynihan DP, Grande DA, Potter HG, Pleshko N Evaluation of Early Osteochondral Defect Repair in a Rabbit Model Utilizing Fourier Transformâ€“Infrared Imaging Spectroscopy, Magnetic Resonance Imaging, and Quantitative T2 Mapping. Tissue Engineering Part C: Methods 16:355-364

59. Bi X, Yang X, Bostrom M, Bartusik D, Ramaswamy S, Fishbein K, Spencer R, Camacho N (2007) Fourier transform infrared imaging and MR microscopy studies detect compositional and structural changes in cartilage in a rabbit model of osteoarthritis. Analytical and Bioanalytical Chemistry 387:1601-1612

60. Qian K. Kang JCL, Helen E. Gruber, Yueheui H.An Histological techniques for decalcified bone and cartilage. In:

61. Landis JR, Koch GG (1977) The Measurement of Observer Agreement for Categorical Data. Biometrics 33:159-174

62. West PA, Torzilli PA, Chen C, Lin P, Camacho NP Fourier transform infrared imaging spectroscopy analysis of collagenase-induced cartilage degradation.

63. West PA, Bostrom, M.P., Torzilli, P.A., and Camacho, N.P (2004) Fourier Transform Infrared Spectral Analysis of Degenerative Cartilage: An Infrared Fiber Optic Probe and Imaging Study. Applied Spectroscopy 58:376-381

64. Depalma AF, McKeever CD, Subin DK (1966) 23 Process of Repair of Articular Cartilage Demonstrated by Histology and Autoradiography With Tritiated Thymidine. Clinical Orthopaedics and Related Research 48:229-242

65. Nam EK, Makhsous M, Koh J, Bowen M, Nuber G, Zhang L-Q (2004) Biomechanical and Histological Evaluation of Osteochondral Transplantation in a Rabbit Model. The American Journal of Sports Medicine 32:308-316

66. Johnson LL (1986) Arthroscopic abrasion arthroplasty historical and pathologic perspective: Present status. Arthroscopy: The Journal of Arthroscopic & Related Surgery 2:54-69

67. Mankin HJ (1982) The response of articular cartilage to mechanical injury. J Bone Joint Surg Am 64:460-466

68. Diem M, Papamarkakis K, Schubert J, Bird B, Romeo MJ, Miljkovi M (2009) The Infrared Spectral Signatures of Disease: Extracting the Distinguishing

Spectral Features Between Normal and Diseased States. Appl. Spectrosc. 63:307A-318A

69. Jamin N, Miller L, Moncuit J, Fridman W-H, Dumas P, Teillaud J-L (2003) Chemical heterogeneity in cell death: Combined synchrotron IR and fluorescence microscopy studies of single apoptotic and necrotic cells. Biopolymers 72:366-373

70. Jackson M, Choo L-P, Watson PH, Halliday WC, Mantsch HH (1995) Beware of connective tissue proteins: Assignment and implications of collagen absorptions in infrared spectra of human tissues. Biochimica et Biophysica Acta (BBA) - Molecular Basis of Disease 1270:1-6

71. Bi X, Yang X, Bostrom MPG, Camacho NP (2006) Fourier transform infrared imaging spectroscopy investigations in the pathogenesis and repair of cartilage. Biochimica et Biophysica Acta (BBA) - Biomembranes 1758:934-941

APPENDIX

Appendix A: Protocols

Alcian blue and Hematoxylin staining

Deparaffinization

1. Immerse the tissue sample in Histoclear – 5min.
2. Second immerse in Histoclear – 5 min.
3. First immerse in 100% Ethanol – 3 min.
4. Second immerse in 100% Ethanol – 3min.
5. First immerse in 95% Ethanol – 3 min.
6. Second immerse in 95% Ethanol – 3 min.
7. Immerse in 70% Ethanol – 3 min.
8. Immerse in 50% Ethanol – 3 min.
9. Immerse in dehydrates H_2O till ready for staining.

Alcian Blue and Hematoxylin Staining

1. Immerse in dehydrated H_2O – 2 min.
2. Immerse in 3% Acetic acid – 3 min.
3. Immerse in Alcian blue – 7 min.
4. First immerse in acid alcohol – 2 min.
5. Second immerse in acid alcohol – 2 min.
6. Immerse in tap water – 1 min.
7. Immerse in Hematoxylin – 5 min.
8. Wash in tap water until water is clear.

9. Immerse in Eosin – 10-20 seconds.
10. First immerse in 95% alcohol – 1 min.
11. Second immerse in 95% alcohol – 1 min.
12. Immerse in 100% - 1 min.
13. Immerse in Histoclear – 1 min.
14. Immerse the sections in another Histoclear which will act as a hold.
15. Mount cover slip with Permont.

DAB Immunohistochemistry protocol

(Select a positive control tissue and include a negative control = include all steps except 1% BSA in PBS w/0.1% Tween will replace the addition of primary antibody in neg. control)

1. **Remove Paraffin and Rehydrate specimen**
    a. Histoclear 2 X 3 min (start paraffin only a-f)
    b. 100% EtOH 2 X 3 min
    c. 95% EtOH 2X 3 min
    d. 75% EtOH 3 min
    e. 50% EtOH 3 min
    f. dH_2O 3 min
    g. PBS 3 min (Hold) (start Cytospins and Frozen) 4% Paraformaldehyde fixation

2. **Antigen-Retrieval (AR)**

a. Boil AR solution 2 min microwave

b. Immerse Slides 10 min

c. Transfer to PBS 5 min

d. Repeat 2 x if paraffin

e. When doing hyaluronidase digestion, replace this step ith it (incubate half hour at 37^{o}C)

3. Permeablization

a. 0.5% Triton X-100 in PBS

b. Incubate at room temperature 10 min

c. Rinse with PBS 3X 2 min

4. Inhibition of endogenous peroxidases

a. 3% H2O2 in Methanol 5 min (15 ml 30% H2O2 + 135 ml Methanol)

b. Rinse with PBS 3 X 2 min

5. Blocking

a. Remove excess liquid with kimwipe

b. 4% BSA in PBS w/0.1 % Tween 20

c. Incubate at room temperature for at least 1 hour

d. Rinse with PBS 3 X 2 min

6. **Primary Antibody Application (Dako cat # A0398 Polyclonal Rabbit anti-human 1:300)**
   a. Bring desired antibody to appropriate dilution with 1% BSA in PBS w/0.1% Tween
   b. Remove excess liquid with kimwipe
      (1) Wipe excess liquid from the back and the sides of the slide
      (2) Wipe top of slide around the tissue removing excess liquid
   c. Apply approximately 100 µl to each specimen (less needed for smaller specimen)
   d. Parafilm cover slip each side
      (1) Use smallest possible size parafilm
      (2) Make sure no bubbles are present
   e. Incubate overnight at $4^{o}C$
   f. Remove parafilm carefully (do not disturb tissue)
   g. Rinse with PBS 3 X 2 min

7. **Secondary Antibody Application (Biotinylated Anti-mouse 1:200) (fridge) (1 drop to 1 ml)**
   a. Bring desired biotinylated antibody to appropriate dilution with 1% BSA in PBS w/0.1% Tween (1:200 dilution of secondary Ab; 5µl into 995µl)
   b. Remove excess liquid with kimwipe
   c. Apply approximately 100µl to each specimen (less needed for smaller specimens)

d. Parafilm cover each slide

    (1) Use smallest possible size parafilm

    (2) Make sure no bubbles are present

e. Incubate at room temperature for 1 hour

f. Rinse with PBS 3 X 2 min

8. Visualization

a. Remove excess liquid with kimwipe

b. Apply a few drops of Horseradish Peroxidase to each slide

c. Incubate at room temperature for 30 min

d. Rinse with PBS 3 X 2 min

e. Apply a few drops of DAB to each slide (Do not place on ice; substrate should be at, at least room temperature)

f. Incubate at room temperature for 10-20 minutes, checking microscopically for positive indications of reaction (golden brown)

g. Rinse with tap H_2O for 5 min.

9. Counter stain with Hematoxylin

a. Rinse with PBS 2 min

b. Hematoxylin 30 sec (end section on slide) (1:1 dilution)

c. Rinse with tap water X 2 or until rinse is clear

d. Dehydrate specimen in 70% ETOH X 2 for 1 min each

e. 95% ETOH X 2 for 1 min each

f. 100% ETOH for 1 min

g. Histoclear 1 min or Xylene (leaves slides in solution until ready to coverslip)

10. Apply Permount and coverlsip

Appendix B: Histological and Immunohistochemical Images

2 Week Samples

Sample 54 Grade11.75

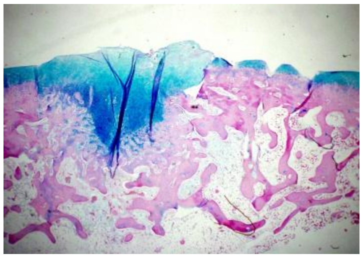

Type I collagen

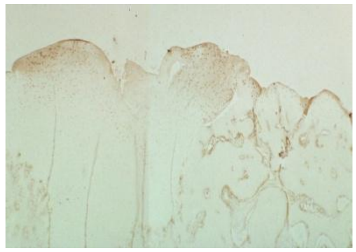

Type II collagen

Sample 46 Grade 9.25

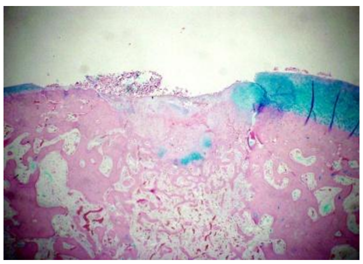

Type I

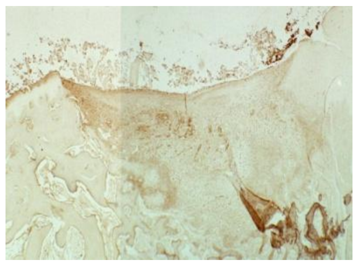

Type II

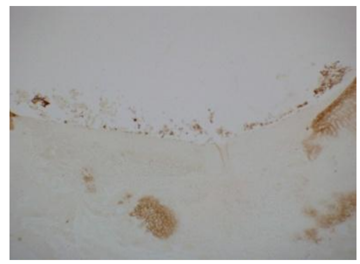

Sample Grade 12

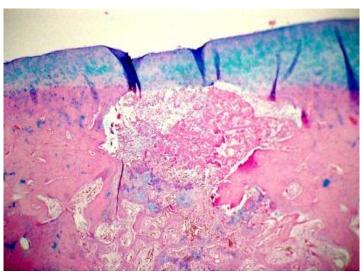

Type I

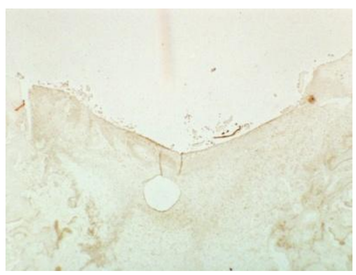

Type II

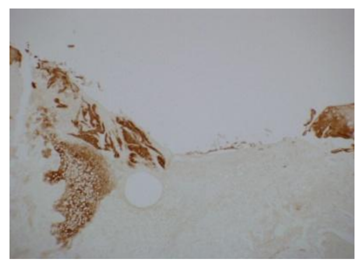

Sample 44 Grade 14.5

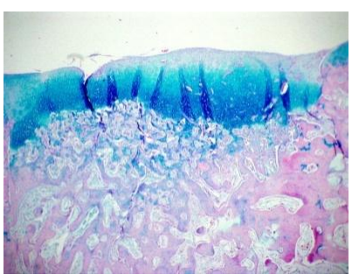

Type I

Type II

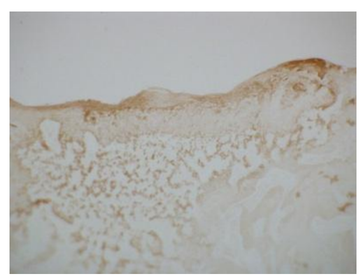

4 Week Samples

Sample 45 Grade 14 **Type I** **Type II**

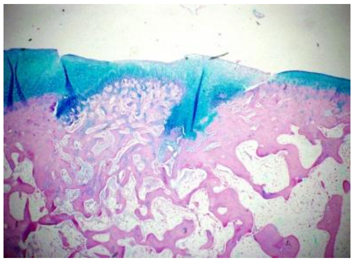 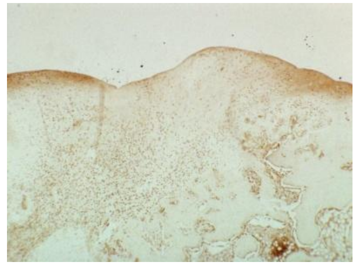 

Sample 39 Grade 6 **Type I** **Type II**

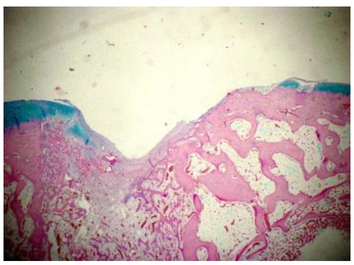 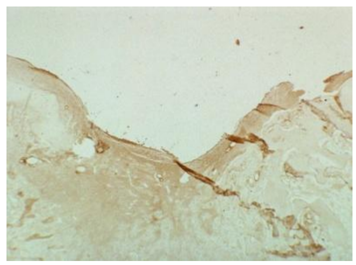 

Smple 34 Grade 16 **Type I** **Type II**

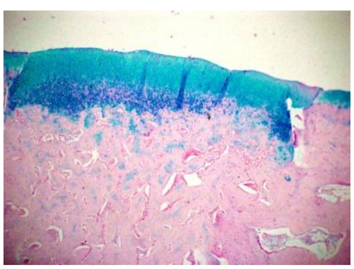 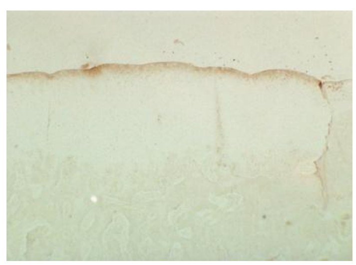 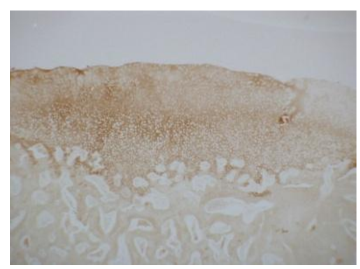

6 Week Samples

Sample 24 Grade 15	Type I	Type II
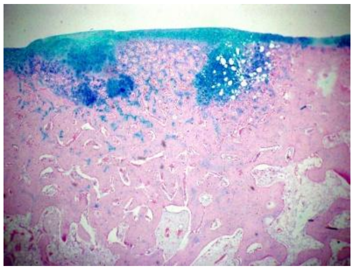	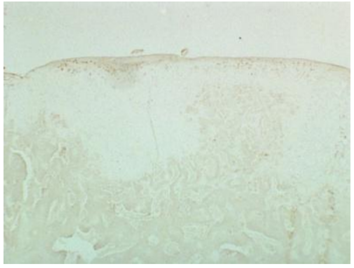	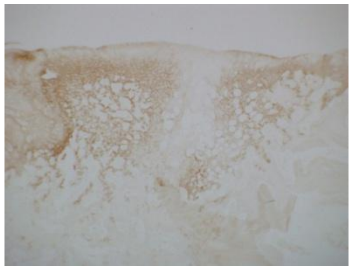
Sample 27 Grade 15	**Type I**	**Type II**
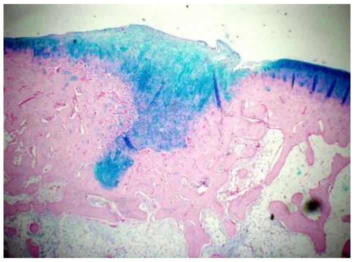	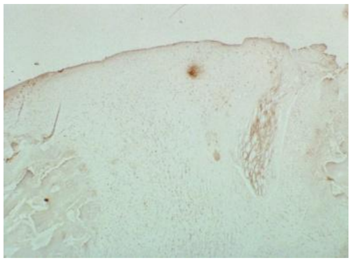	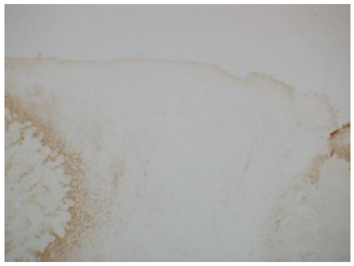
Sample 30 Grade 13.75	**Type I**	**Type II**
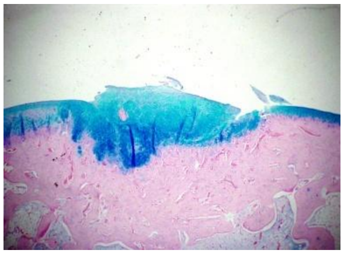	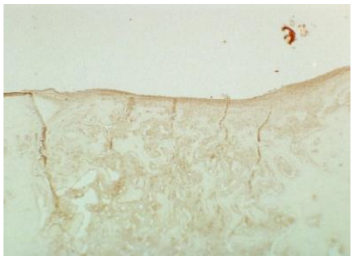	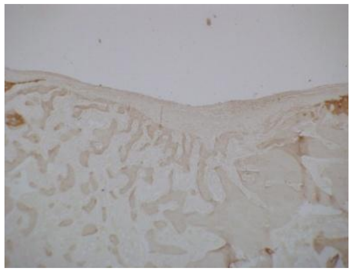

8 Week Samples

Sample 29 Grade 16.5 **Type I** **Type II**

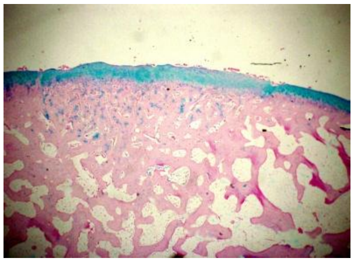
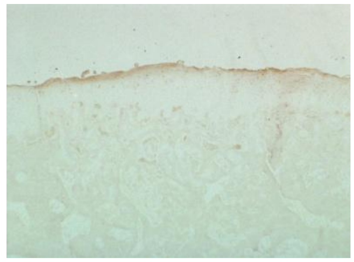
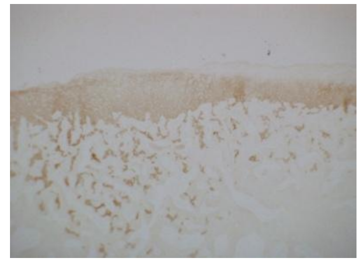

Sample 33 Grade 13 **Type I** **Type II**

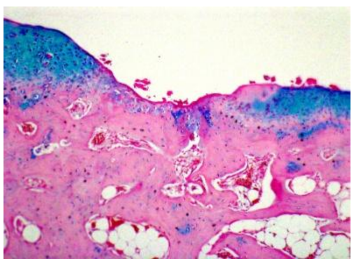
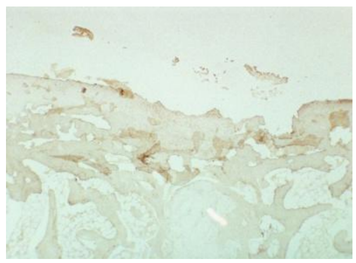


Sample 32 Grade 17.5 **Type I** **Type II**

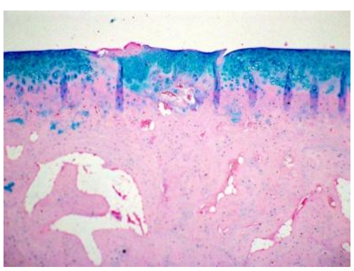
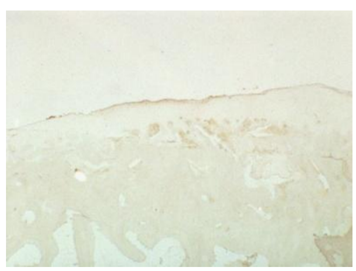
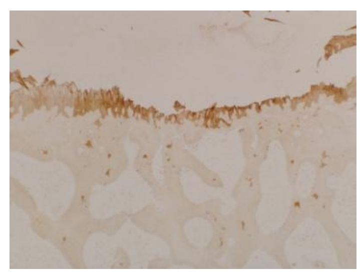

Sample 23 Grade 13.5 **Type I** **Type II**

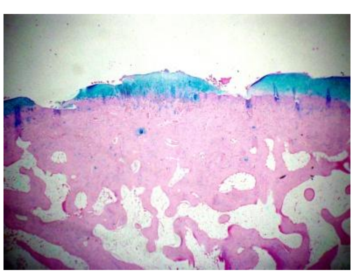
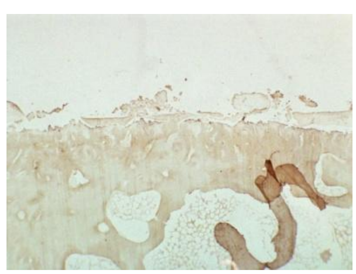


12 Week Samples

Sample 22 Grade 9 | **Type I** | **Type II**

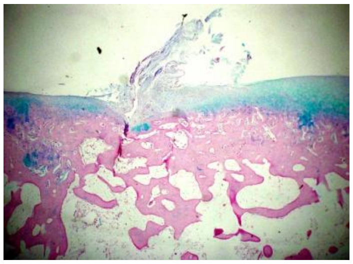
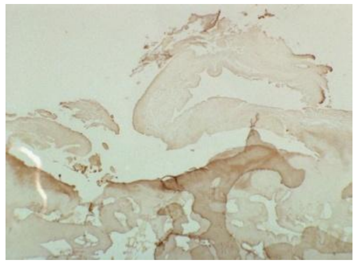
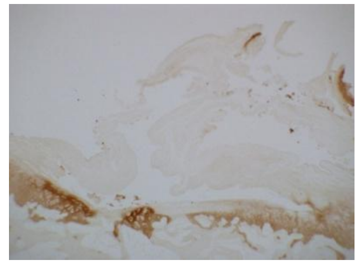

Sample 35 Grade 9.75 | **Type I** | **Type II**

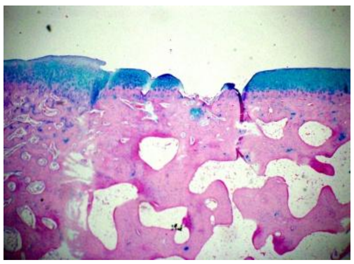

Sample 31 Grade 11.5 | **Type I** | **Type II**

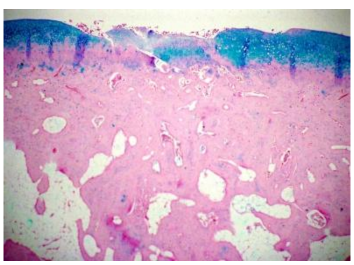
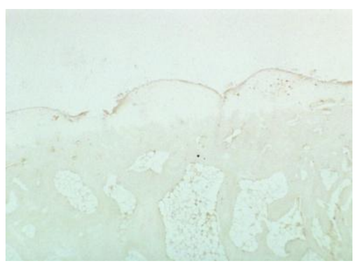
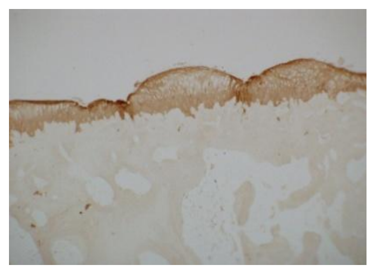

Sample 28 Grade 14 | **Type I** | **Type II**

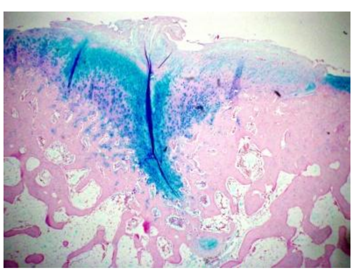
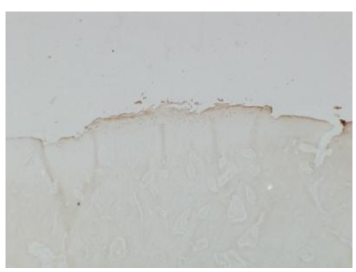
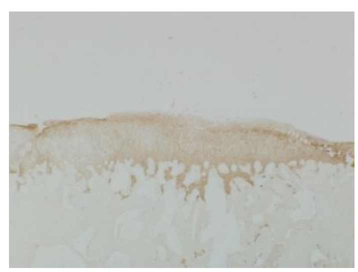

16 Week Samples

Sample 19 Grade 21

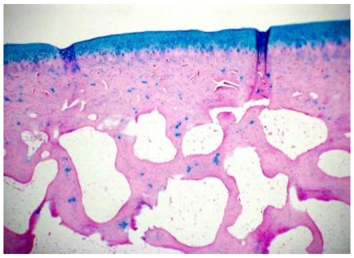

Type I

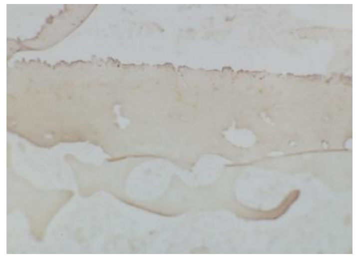

Type II

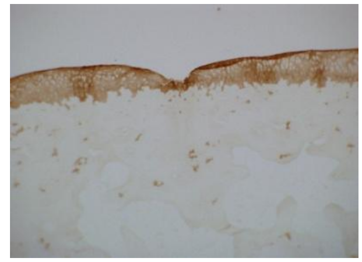

Sample 16 Grade 18

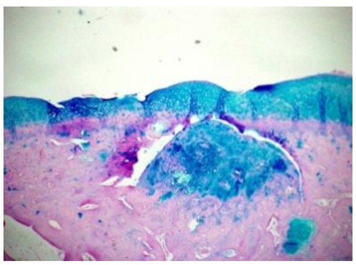

Type I

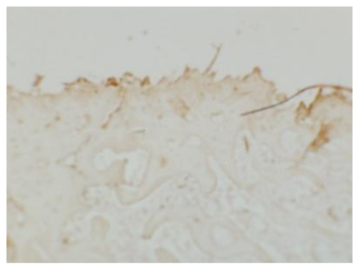

Type II

Sample 10 Grade 15.75

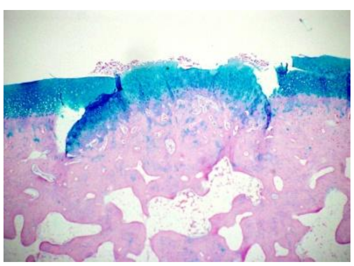

Type I

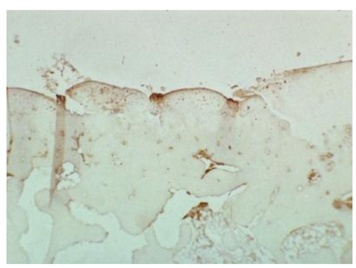

Type II

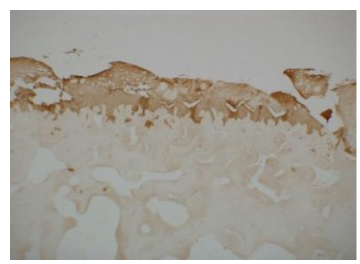

Appendix C: IR Images

2 Week Samples

Sample 46

Original Image

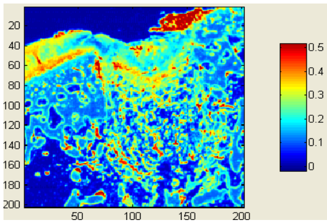

Spectrum

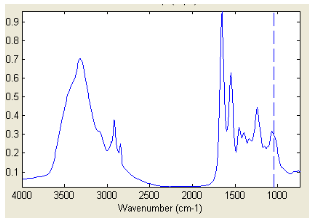

Normal Tissue

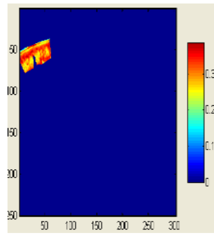

Repair Tissue

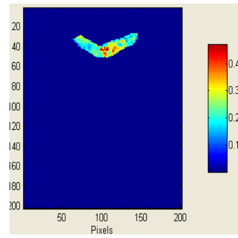

Masked Repair Tissue

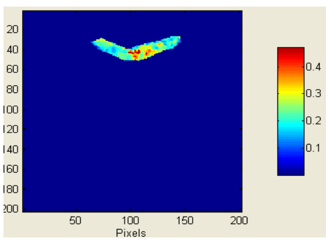

Amide I

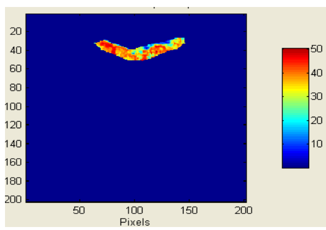

PG

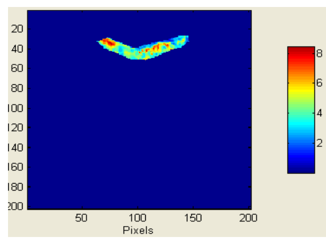

PG /Am I

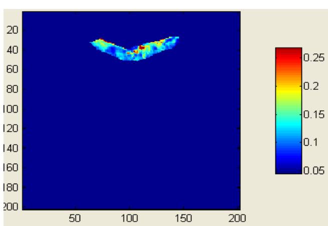

Collagen Integrity(1338/Am II)

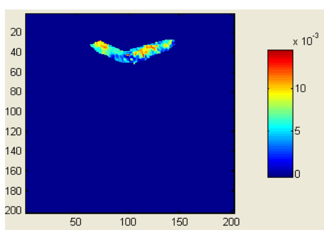

Orientation

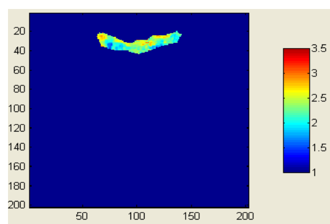

Sample 44

Original Image

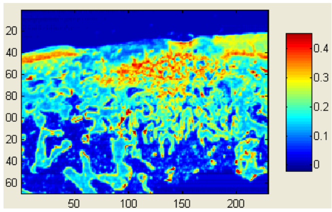

Spectrum

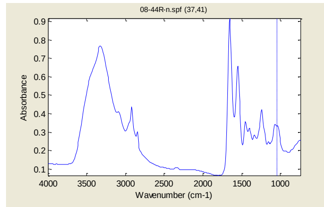

Normal Tissue

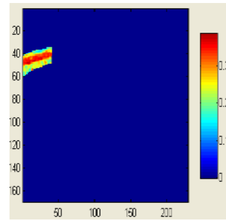

Repair Tissue

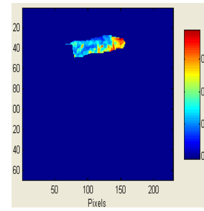

Masked Repair Tissue

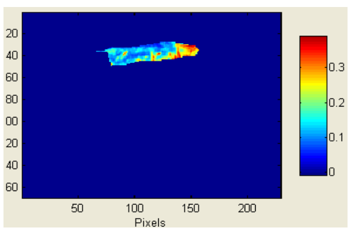

Amide I

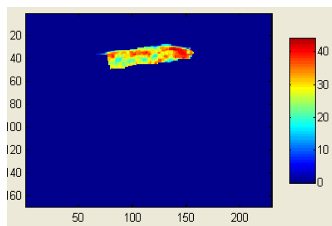

PG

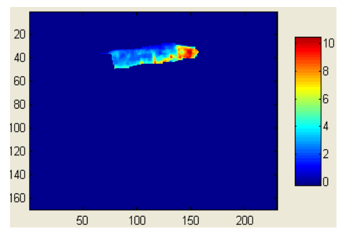

PG /Am I

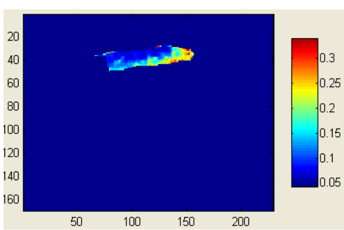

Collagen Integrity(1338/Am II)

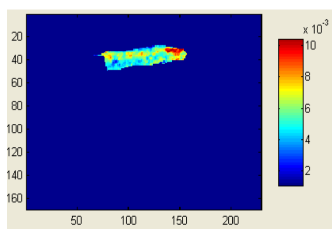

Orientation

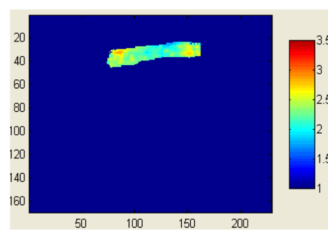

Sample 50

Original Image

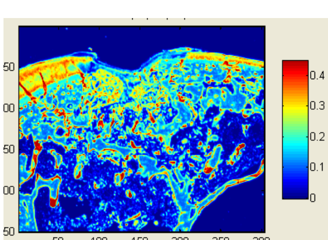

Spectrum

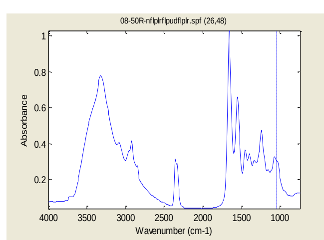

Normal tissue

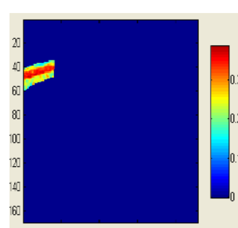

Repair Tissue

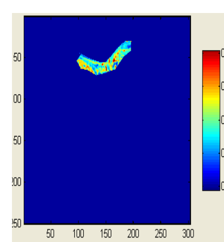

Masked Repair Tissue **Amide I** **PG**

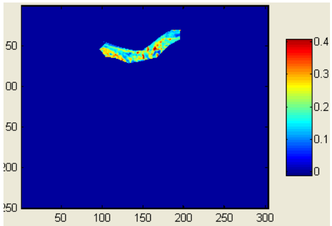

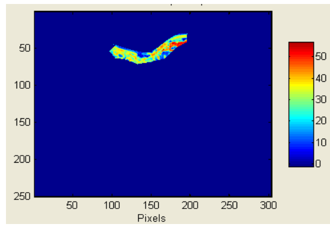

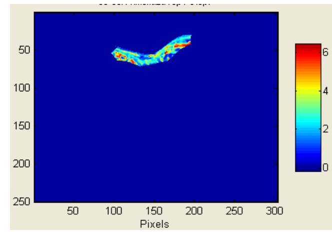

PG /Am I **Collagen Integrity(1338/Am II)** **Orientation**

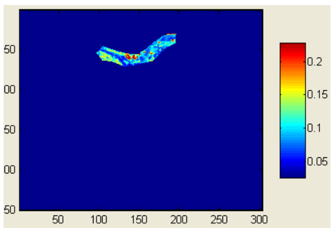

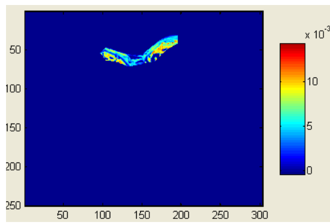

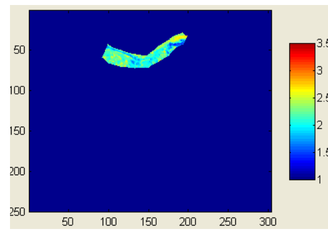

Sample 48

Original Image **Spectrum** **Normal tissue** **Repair Tissue**

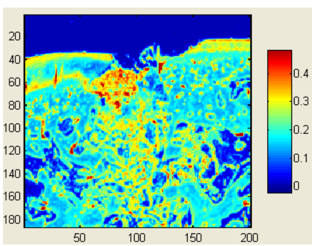

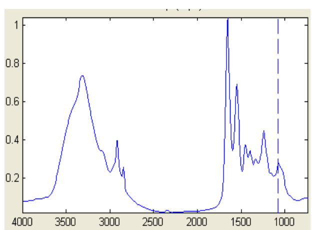

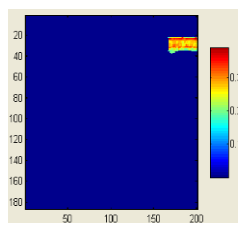

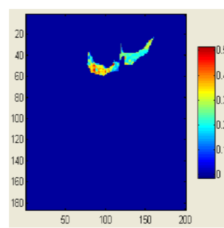

Masked Repair Tissue **Amide I** **PG**

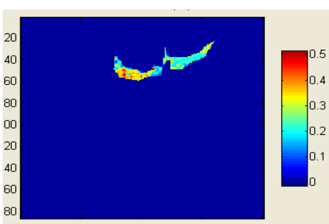

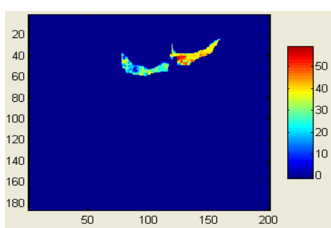

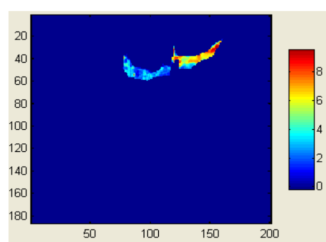

PG / Am I

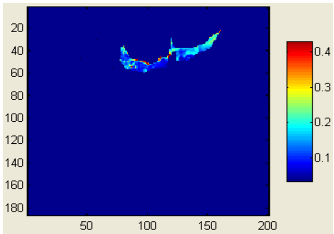

Collagen Integrity(1338/Am II)

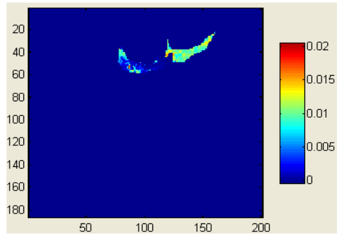

Orientation

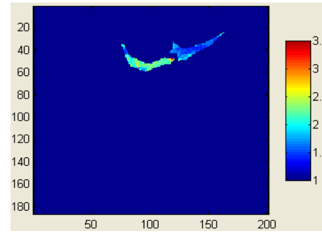

Sample 54

Original Image

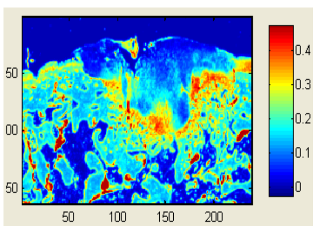

Spectrum

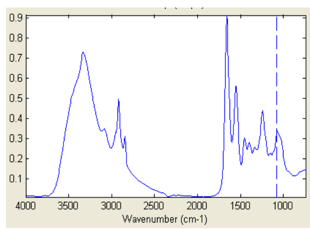

Normal tissue

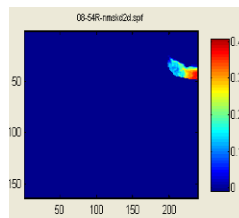

Repair Tissue

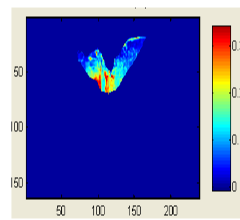

Masked Repair Tissue

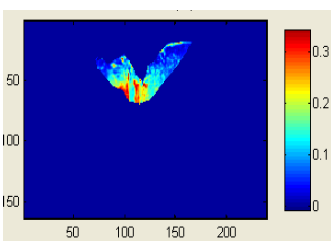

Amide I

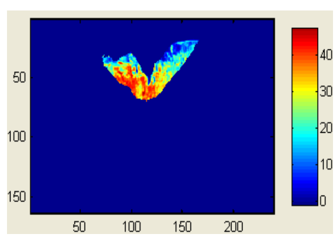

PG

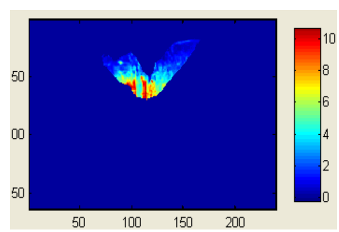

PG / Am I

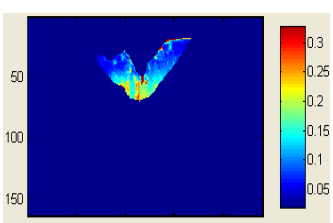

Collagen Integrity(1338/Am II)

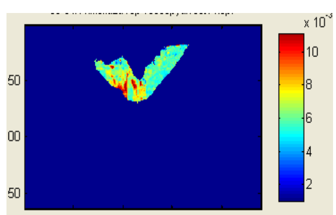

Orientation

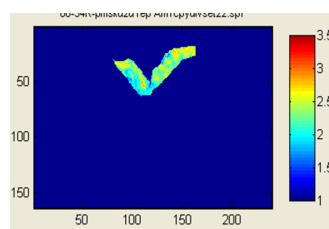

4 Week Samples

Sample 34

Original Image

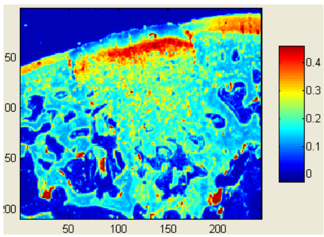

Spectrum

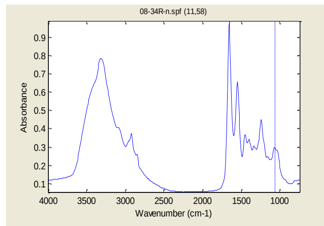

Normal tissue

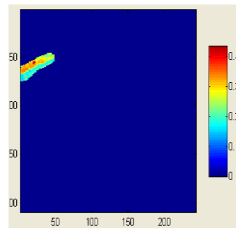

Repair Tissue

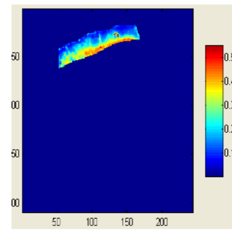

Masked Repair Tissue

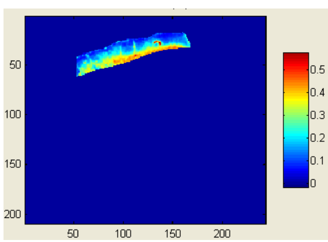

Amide I

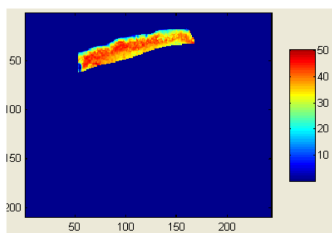

PG

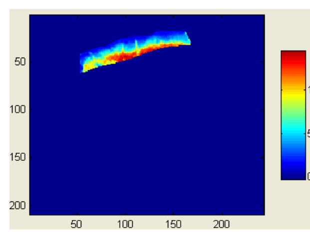

PG / Am I

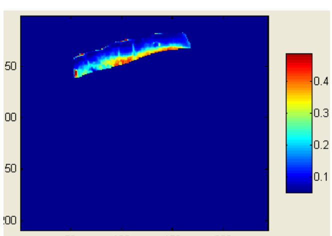

Collagen Integrity(1338/Am II)

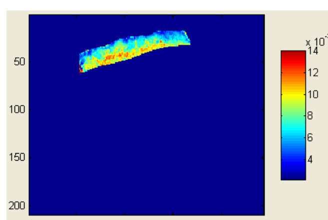

Orientation

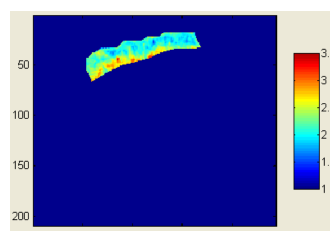

Sample 39

Original Image

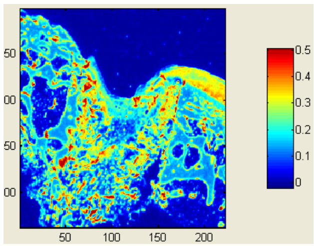

Spectrum

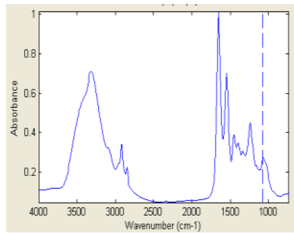

Normal tissue

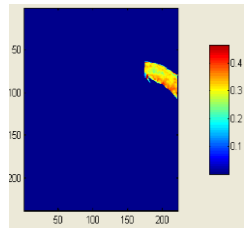

Repair Tissue

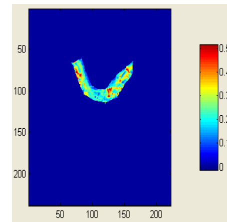

Masked Repair Tissue

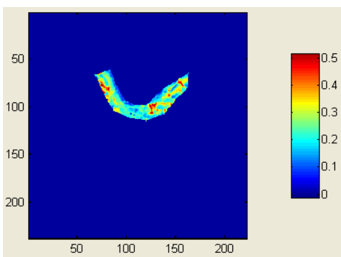

Amide I

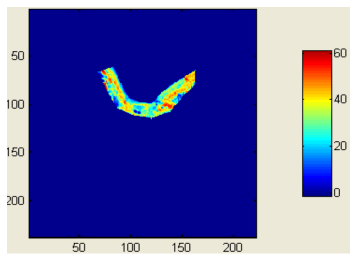

PG

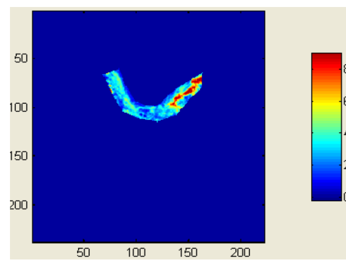

PG / Am I

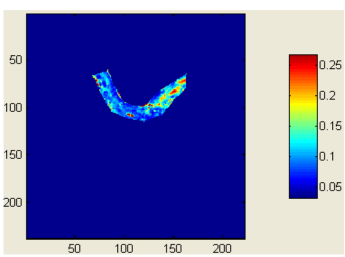

Collagen Integrity(1338/Am II)

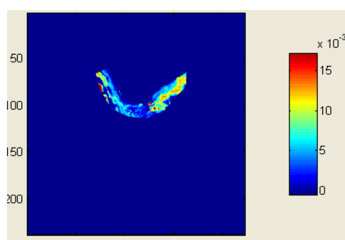

Orientation

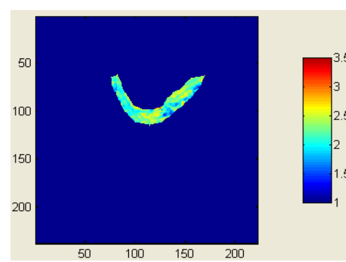

Sample 45

Original Image

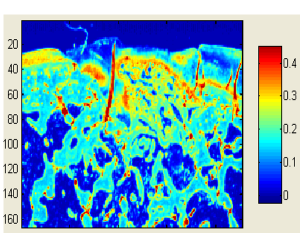

Spectrum

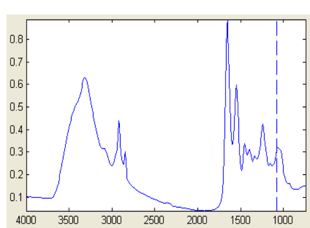

Normal tissue

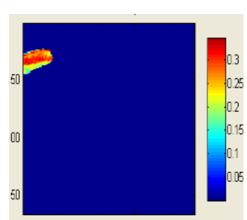

Repair Tissue

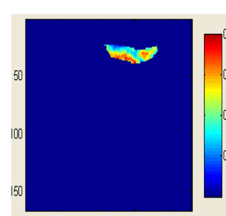

Masked Repair Tissue

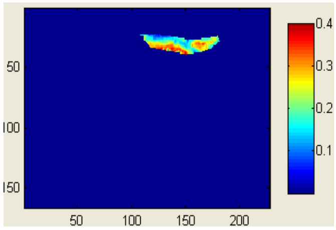

Amide I

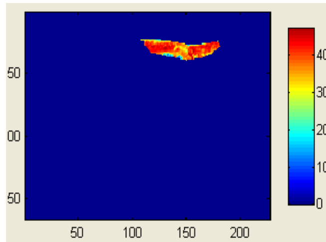

PG

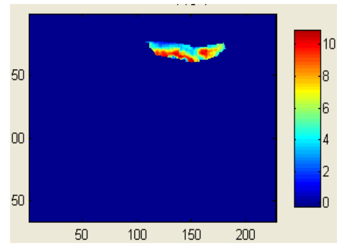

PG / Am I

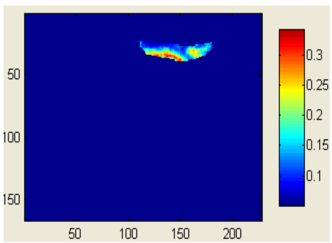

Collagen Integrity(1338/Am II)

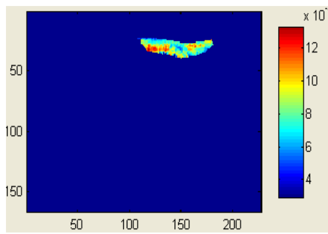

Orientation

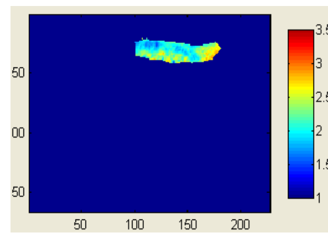

6 Week Samples

Sample 24

Original Image

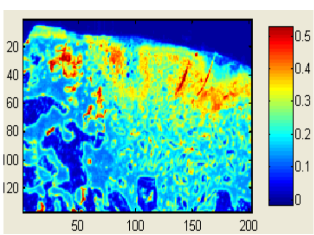

Spectrum

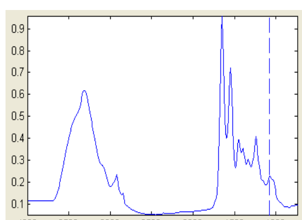

Normal tissue

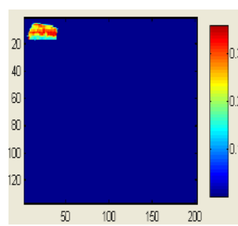

Repair Tissue

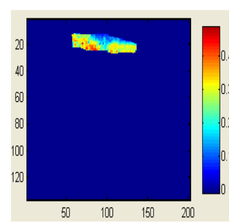

Masked Repair Tissue

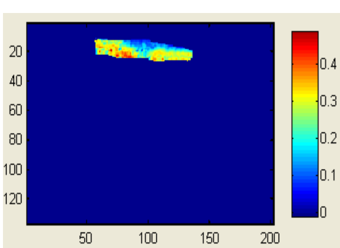

Amide I

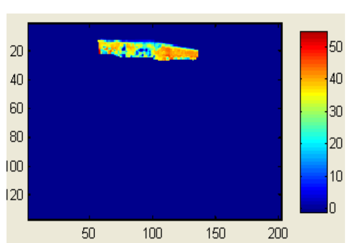

PG

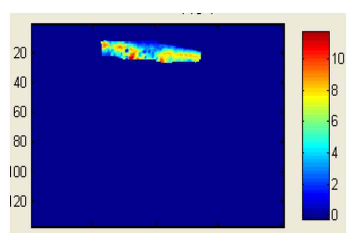

PG / Am I

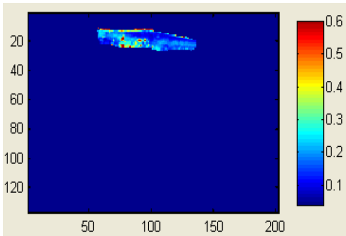

Collagen Integrity(1338/Am II)

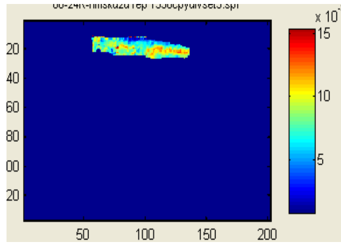

Orientation

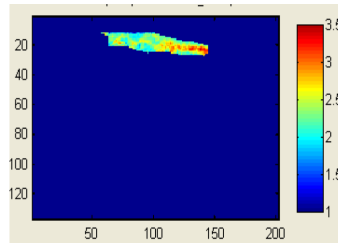

Sample 30

Original Image

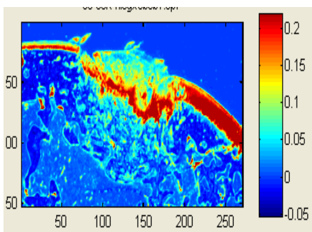

Spectrum

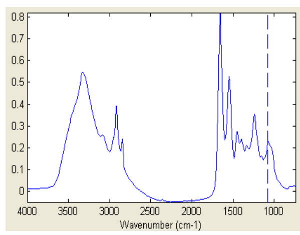

Normal tissue

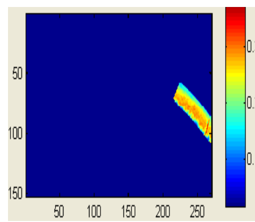

Repair Tissue

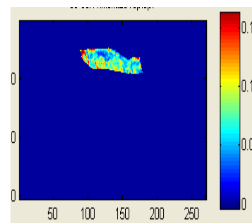

Masked Repair Tissue

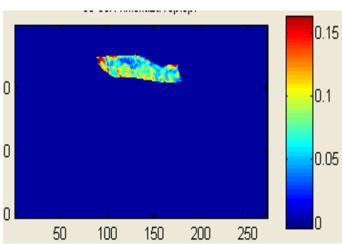

Amide I

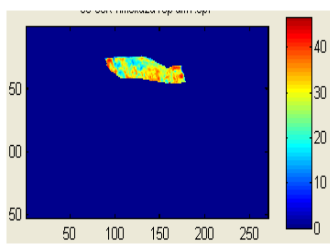

PG

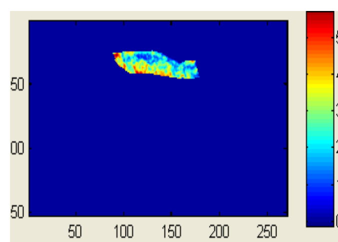

PG / Am I

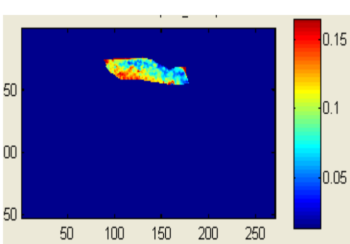

Collagen Integrity(1338/Am II)

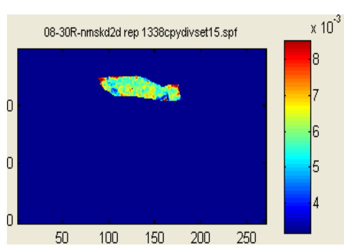

Orientation

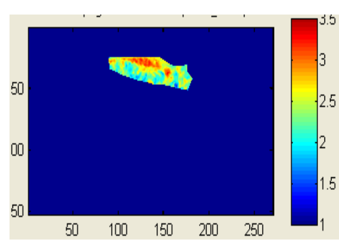

Sample 27

Original Image

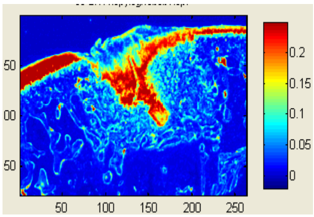

Spectrum

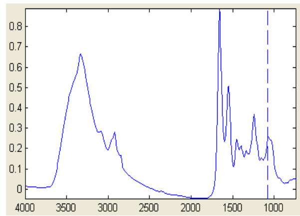

Normal tissue

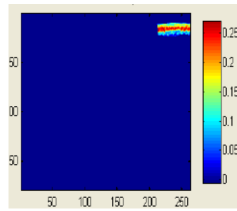

Repair Tissue

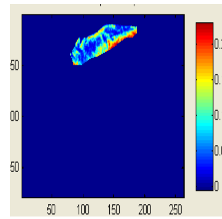

Masked Repair Tissue

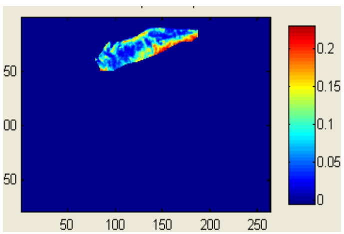

Amide I

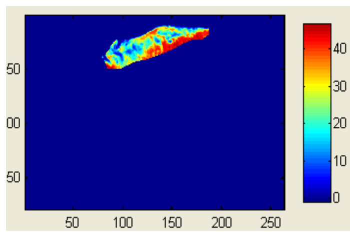

PG

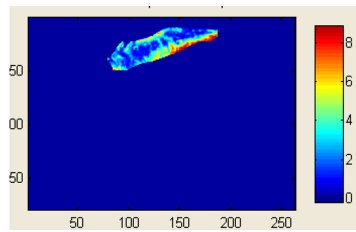

PG / Am I

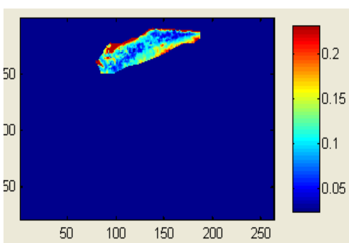

Collagen Integrity(1338/Am II)

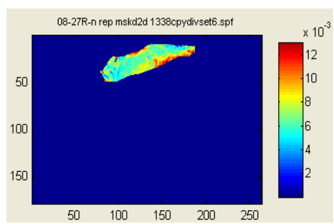

Orientation

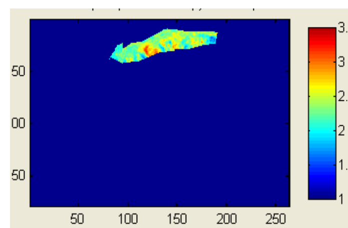

8 Week Samples

Sample

Original Image

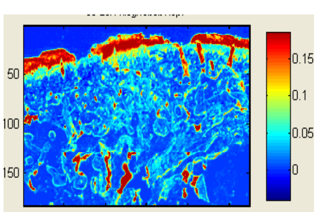

Spectrum

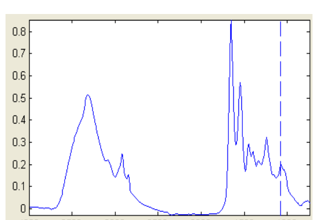

Normal tissue

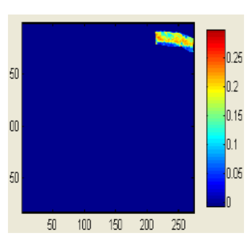

Repair Tissue

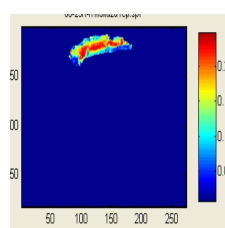

Masked Repair Tissue

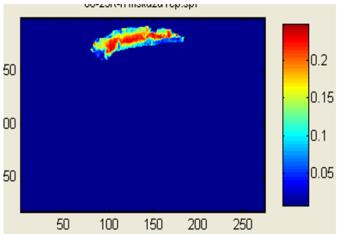

Amide I

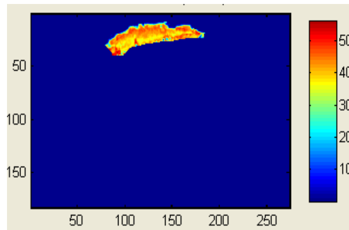

PG

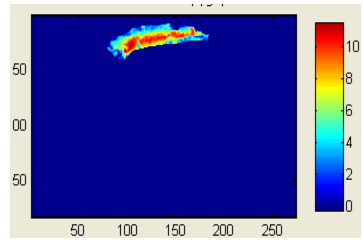

PG / Am I

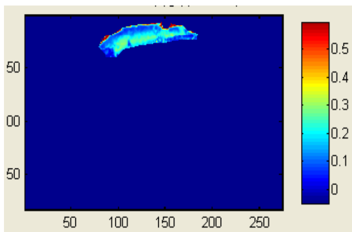

Collagen Integrity(1338/Am II)

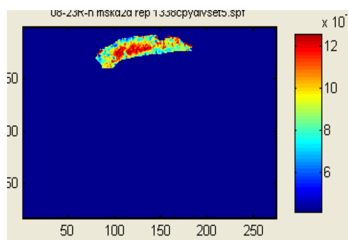

Orientation

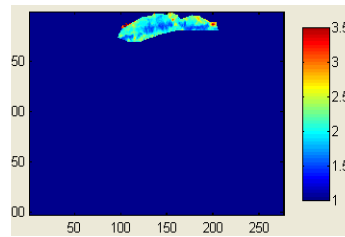

Sample 32

Original Image

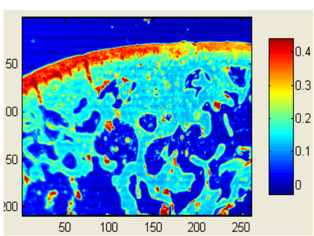

Spectrum

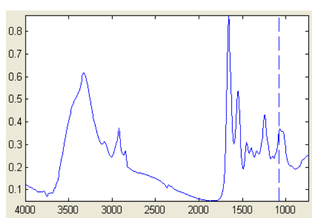

Normal tissue

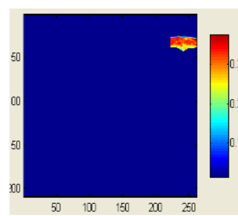

Repair Tissue

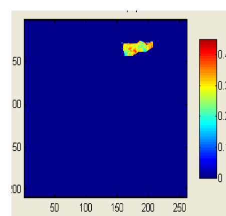

Masked Repair Tissue

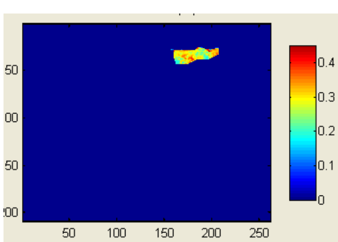

Amide I

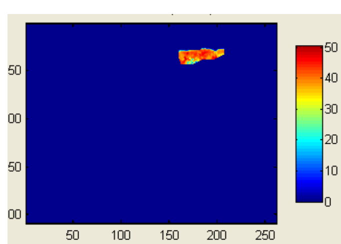

PG

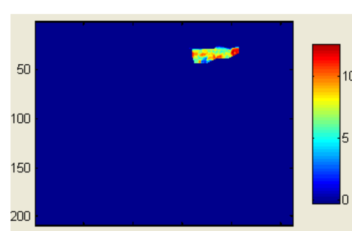

PG / Am I

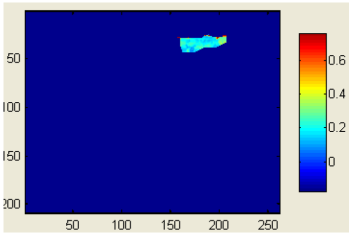

Collagen Integrity(1338/Am II)

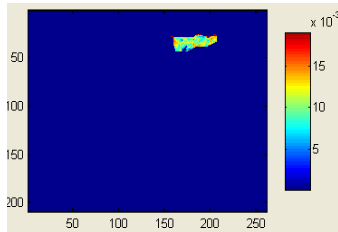

Orientation

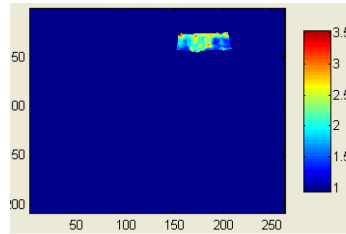

Sample 29

Original Image

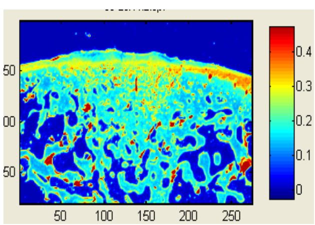

Spectrum

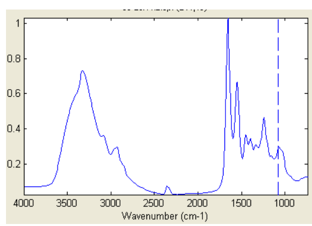

Normal tissue

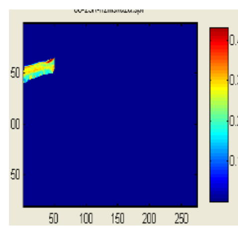

Repair Tissue

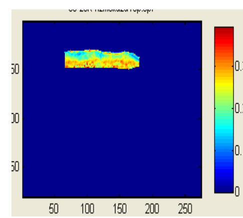

Masked Repair Tissue

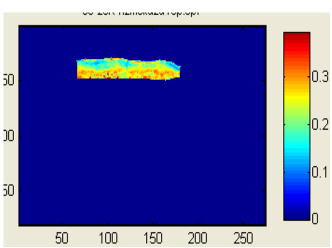

Amide I

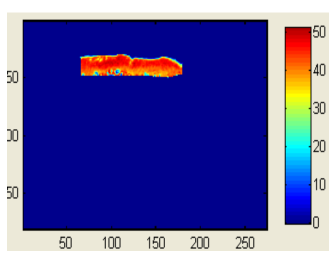

PG

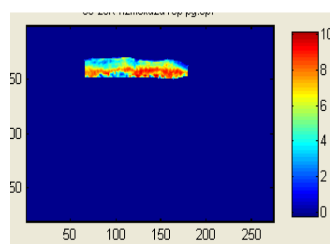

PG / Am I

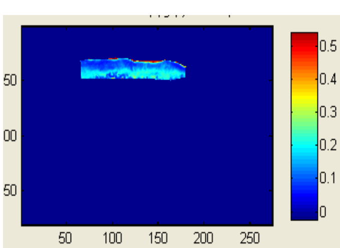

Collagen Integrity(1338/Am II)

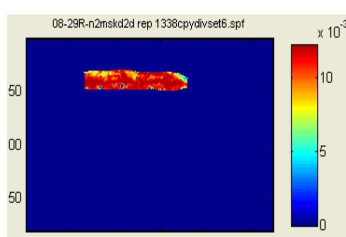

Orientation

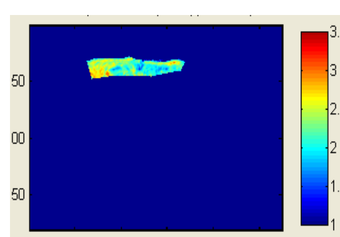

Sample 33

Original Image

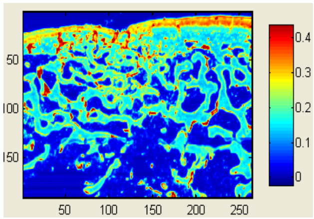

Spectrum

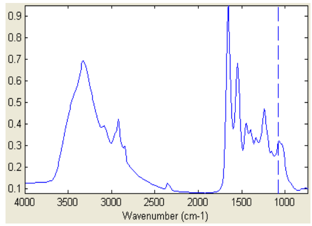

Normal tissue

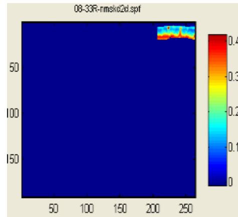

Repair Tissue

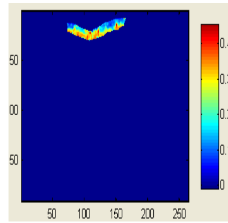

Masked Repair Tissue

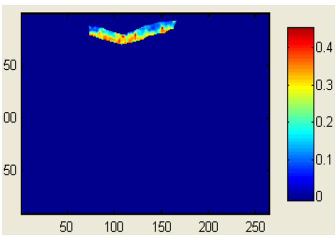

Amide I

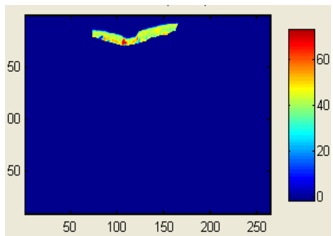

PG

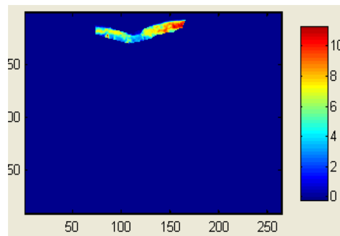

PG / Am I

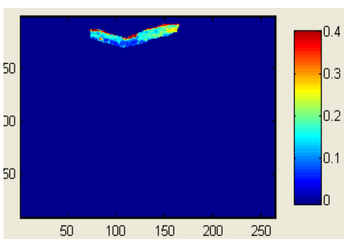

Collagen Integrity(1338/Am II)

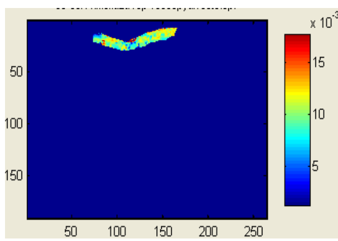

Orientation

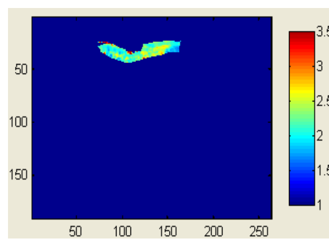

12 Week Samples

Sample 35

Original Image

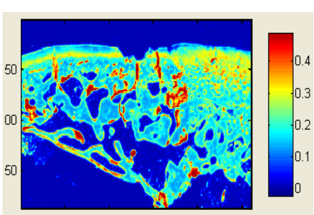

Spectrum

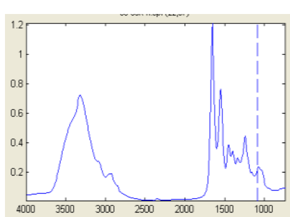

Normal tissue

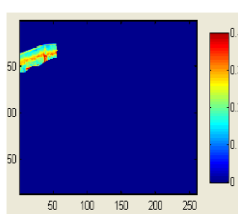

Repair Tissue

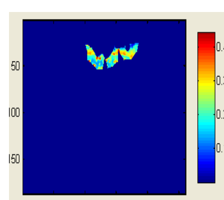

Masked Repair Tissue

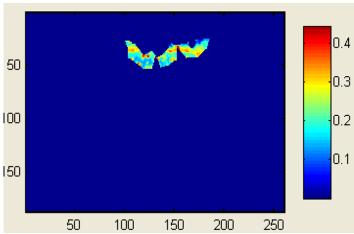

Amide I

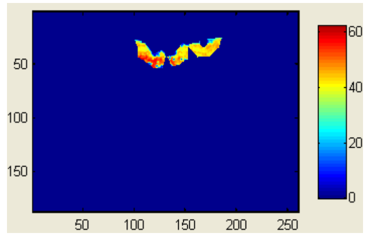

PG

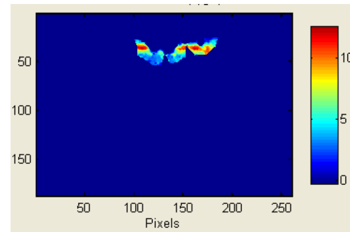

PG / Am I

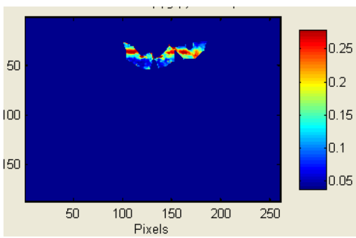

Collagen Integrity(1338/Am II)

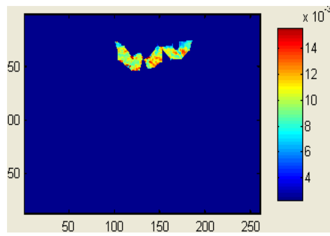

Orientation

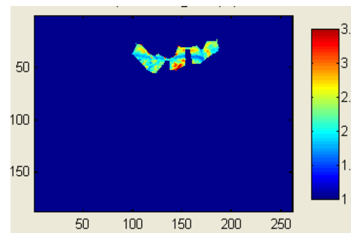

Sample 31

Original Image

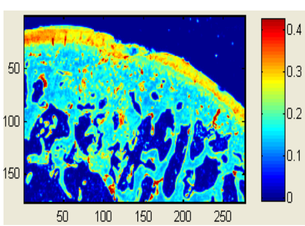

Spectrum

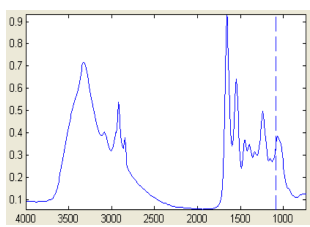

Normal tissue

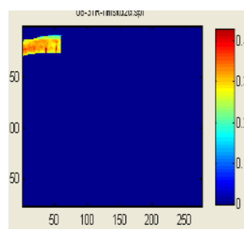

Repair Tissue

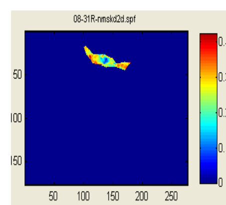

Masked Repair Tissue

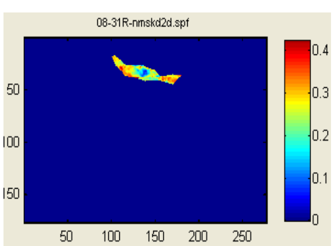

Amide I

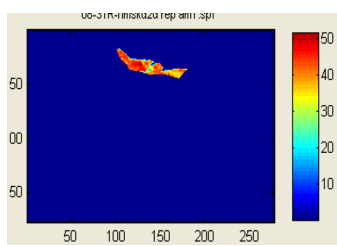

PG

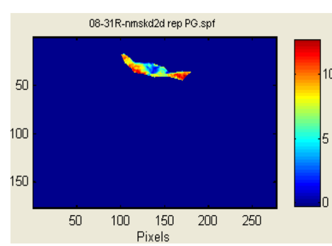

PG / Am I

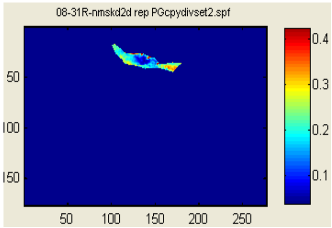

Collagen Integrity(1338/Am II)

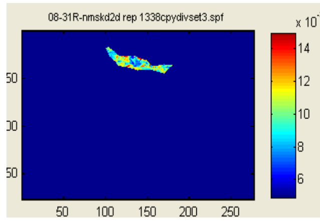

Orientation

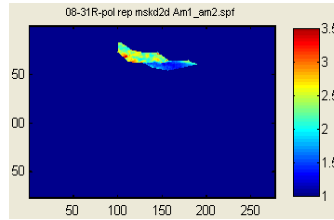

Sample 28

Original Image

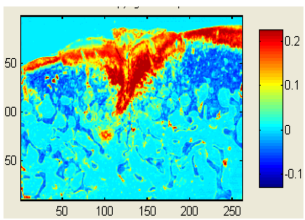

Spectrum

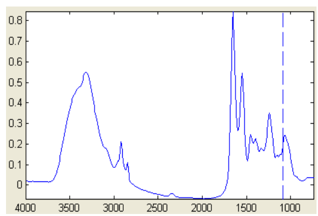

Normal tissue

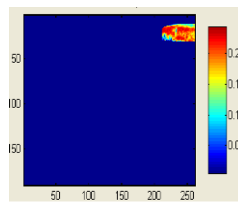

Repair Tissue

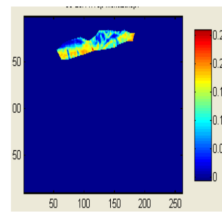

Masked Repair Tissue

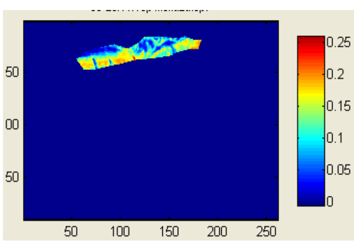

Amide I

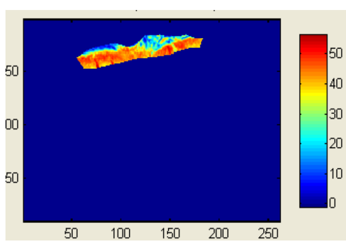

PG

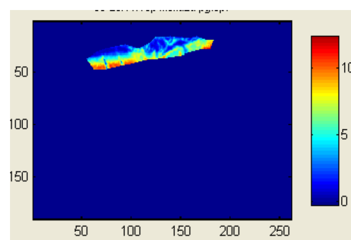

PG / Am I

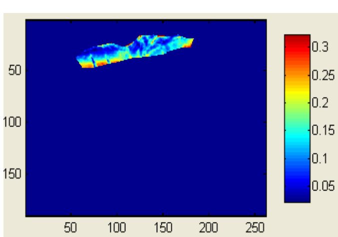

Collagen Integrity(1338/Am II)

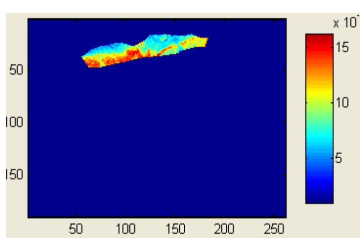

Orientation

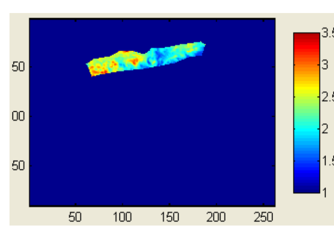

Sample 22

Original Image

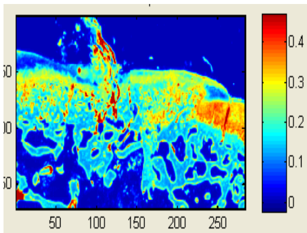

Spectrum

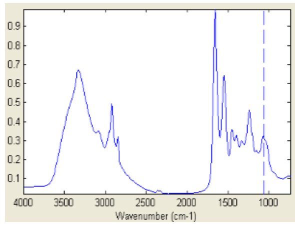

Normal tissue

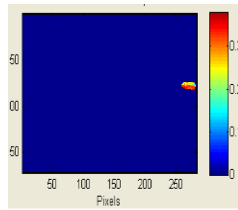

Repair Tissue

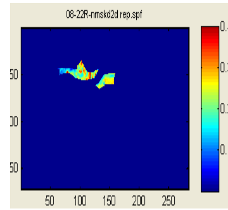

Masked Repair Tissue

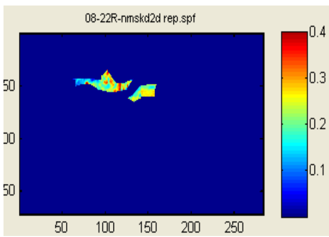

Amide I

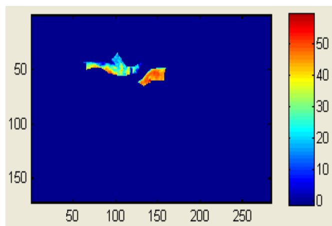

PG

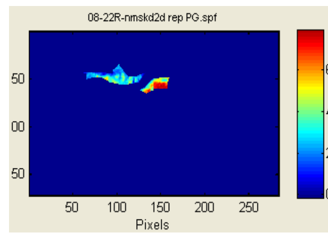

PG / Am I

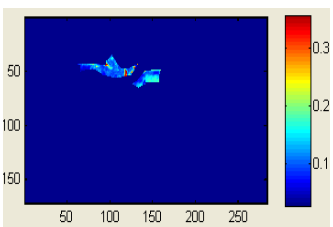

Collagen Integrity(1338/Am II)

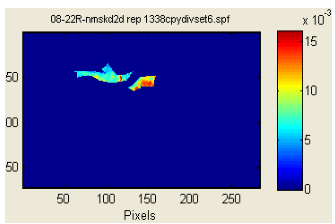

Orientation

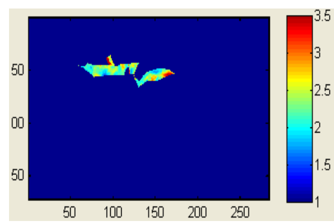

16 Week Samples

Sample 10

Original Image

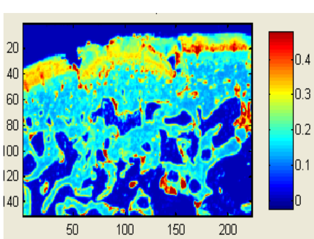

Spectrum

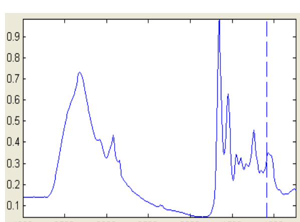

Normal tissue

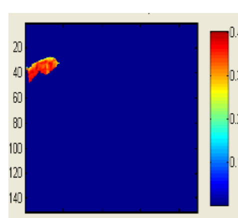

Repair Tissue

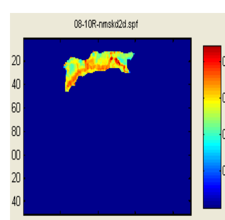

Masked Repair Tissue | **Amide I** | **PG**

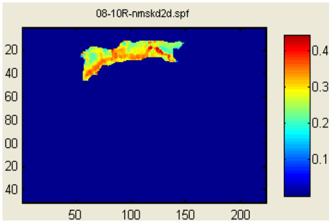

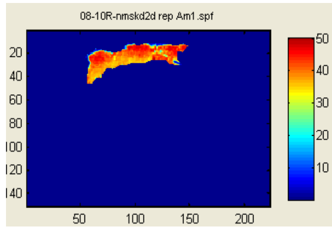

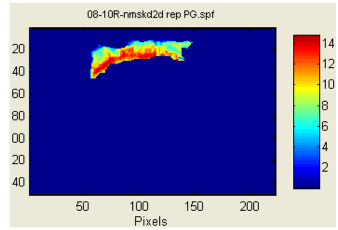

PG / Am I | **Collagen Integrity(1338/Am II)** | **Orientation**

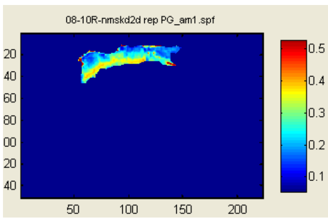

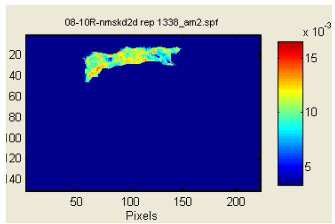

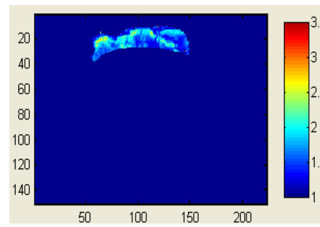

Sample 05

Original Image | **Spectrum** | **Normal tissue** | **Repair Tissue**

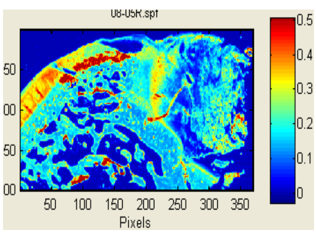

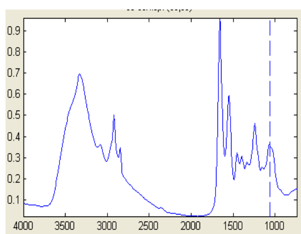

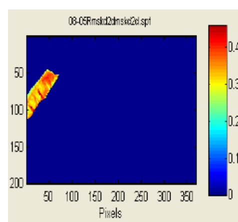

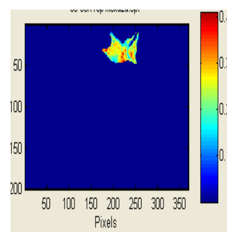

Masked Repair Tissue | **Amide I** | **PG**

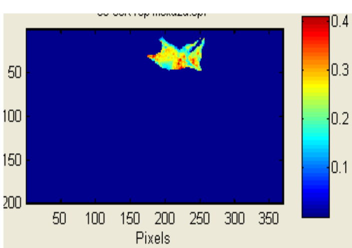

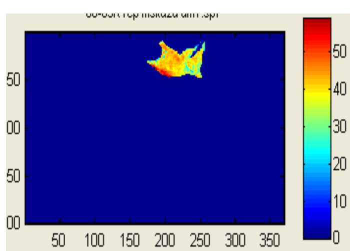

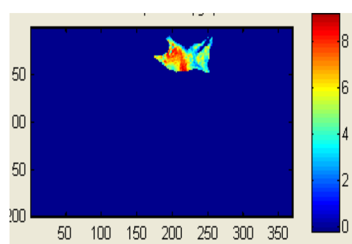

PG / Am I **Collagen Integrity(1338/Am II)** **Orientation**

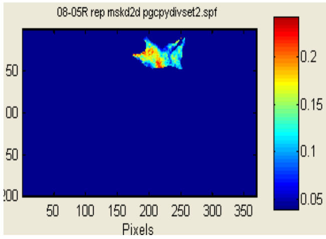

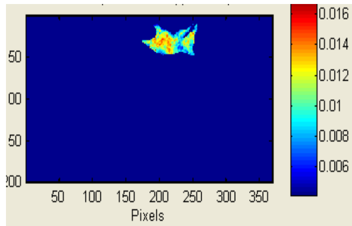

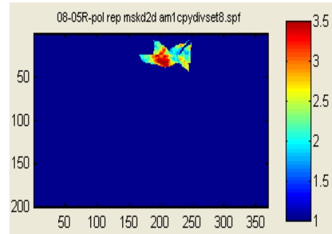

Sample 16

Original Image **Spectrum** **Normal tissue** **Repair Tissue**

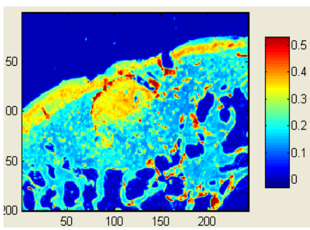

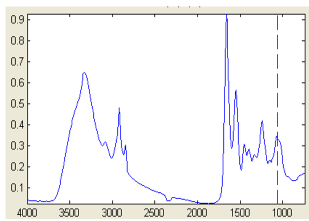

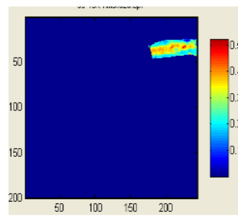

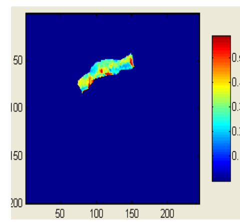

Masked Repair Tissue **Amide I** **PG**

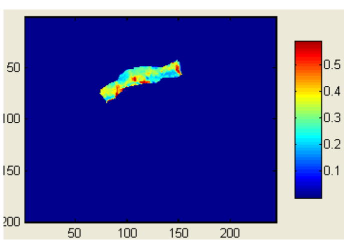

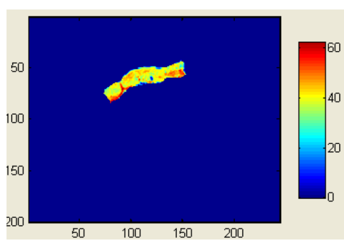

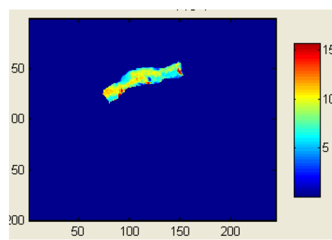

PG / Am I **Collagen Integrity(1338/Am II)** **Orientation**

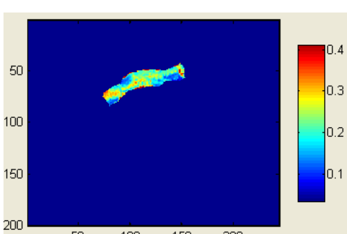

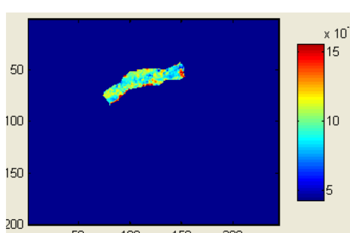

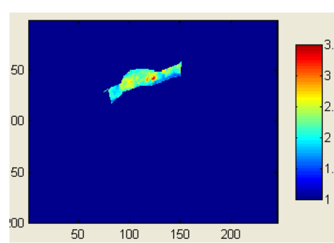

Sample 19

Original Image

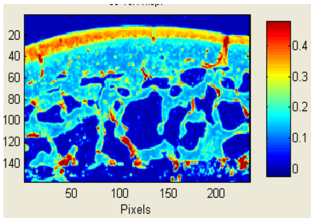

Spectrum

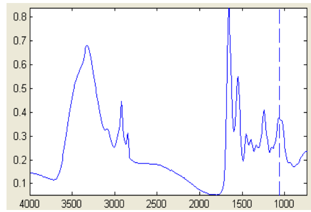

Normal tissue

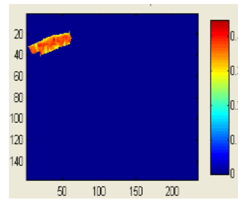

Repair Tissue

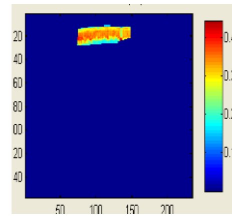

Masked Repair Tissue

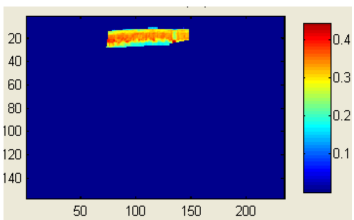

Amide I

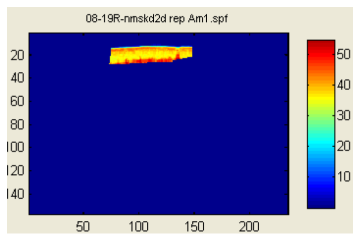

PG

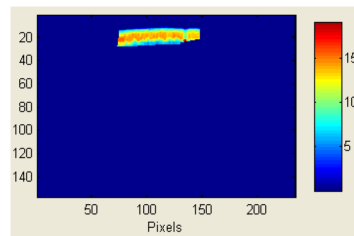

PG / Am I

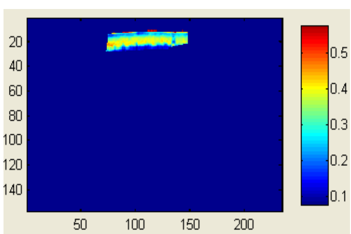

Collagen Integrity(1338/Am II)

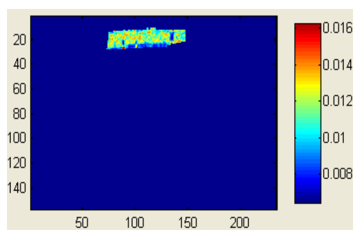

Orientation